NOVEL CO-POLYIMIDE MEMBRANES CONTAINING A SULFONE GROUP FOR CO_2 SEPARATION

Sadiye Velioğlu, M. Göktuğ Ahunbay, S. Birgül Tantekin-Ersolmaz*
Istanbul Technical University, Dept. of Chemical Eng., Maslak, Istanbul 34469, TURKEY
* ersolmaz@itu.edu.tr

Abstract

In this study, three different co-polyimides containing a sulfone group were synthesized and characterized in pursuit of gas separation membrane materials with high CO_2/CH_4 separation performance. The co-polyimides, 6FDA/BTDA-pBAPS (3:1), 6FDA-pBAPS/mPDA (3:1) and 6FDA-pBAPS/DABA (3:1), were identified as promising structures with above upper bound permeability and selectivity values in our previous study based on a group contribution method. Measured permeability coefficients for O_2, N_2, CO_2, and CH_4 gases were in good agreement with the predictions of the group contribution method, confirming that group contribution methods could be used for fast screening of co-polyimides. Molecular simulation techniques also were used to estimate the structural properties (d-spacing, glass transition temperature, fractional free volume, etc.) which were in good agreement with the measured experimental results. Preferential CO_2 sorption sites in co-polyimides were investigated through the analysis of the radial distribution function (RDF), and the available vacancy inside the simulation cell was detected by accessible free volume analysis. RDF results showed that the main interaction with CO_2 arises from the sulfur groups in the pBAPS diamine which increase the sorption coefficient of CO_2. Moreover, the carboxyl group in DABA diamine enables the formation of hydrogen bonds which results in closed packing and decrease in the sorption and permeability coefficients. Experimental and simulated sorption coefficients are in good agreement with each other. The co-polyimides investigated here did not show any plasticization behavior in experiments conducted up to 9 bar.

Keywords: Co-polyimide, sulfone group, permeability, sorption, molecular simulation

1. Introduction

CO_2 separation from gas mixtures is one of the most highly energy demanding processes. One application is CO_2 removal from natural gas. Untreated natural gas generally contains 5-50% CO_2, which causes a reduction in heating value of the gas and corrosion in the transportation pipeline. This high CO_2 content must be reduced to less than 2% in order to meet the pipeline requirement and to increase the heating value. Other common applications include post and pre-combustion CO_2 capture in power plants. Post-combustion CO_2 capture from power plant flue gas (CO_2/N_2) and pre-combustion CO_2 capture from gasified coal synthesis gas (CO_2/H_2) are other industrially important CO_2 separation applications. The most commonly employed conventional method for CO_2 separation is reactive absorption using amines. However, amine-based absorption processes suffer from problems associated with very high energy consumption and large scale equipment which led to high capital and operational costs, and high environmental impact. Membrane based gas separation has great potential to replace the absorption processes due to its superiority associated with high efficiency, reliability, conceptual and operational simplicity, significantly reduced equipment size, low environmental impact, and economy [1,2]. These advantages over conventional separation processes have attracted a lot of attention in terms of research and development, and therefore membrane based gas separation area has progressed considerably since 1980s.

The main focus of a large number of studies is the synthesis of more robust, permeable but still highly selective membranes in order to compete with the current separation technologies [1-3]. Unfortunately, despite the focused attempts at tailoring membrane structure to obtain more attractive separation properties, polymers seem to have reached a productivity/selectivity trade-off [4]. Moreover, the scale-up and commercialization of any promising membrane material developed in the laboratory still remains an issue. For example, for CO_2/CH_4 separation, instead of commercially used cellulose acetate with the selectivity of 15, the use of polyimides with selectivities of 20-25 as membrane material can heat up the membrane market. In fact, membrane technology can deal major blow to many amine plants with the commercialization of membranes with selectivities of 40 and above. However, the sustainable performance of these highly selective membranes for CO_2/CH_4 separation is largely hindered by plasticization. The plasticization phenomenon causes reduction in selectivity and methane productivity, which is undesirable in CO_2 separation from natural gas [5, 6].

Efforts to correlate structures of polymeric membranes with their separation performance (permeability and selectivity) have led to exploration of novel polymeric structures. Among these

polymeric membranes, aromatic polyimides have shown not only high separation performance but also outstanding thermal, mechanical and chemical stability that push the limits of selectivity-permeability trade-off in conventional polymer membrane materials. Other polymers that exhibit improved separation characteristics are TR (thermally rearranged) polymers [7] comprising benzoxazole-phenylene or benzothiazole-phenylene structures in the main chain, and the ladder polymers (PIM-1 and PIM-7) [8].

Polyimides are synthesized by the reaction of two monomers (a dianhydride and a diamine) in a solvent and by dehydration of the polyamic acid formed. If this procedure is carried out with two or more dianhydrides or two or more diamines, then co-polyimides are synthesized. Co-polyimides are promising owing to the fact that they allow us to optimize the separation properties by using two different polyimides which have different permeability and selectivity properties. 6FDA-based co-polyimides are of particular interest since they contain two bulky CF_3 groups, causing an increase of the polymer's fractional free volume (FFV), and thus rise in permeation rates [1]. Moreover, 6FDA-based co-polyimides have the advantage of easy processability as gas separation membrane materials due to their high solubility in various commercial solvents.

Gas transport properties of co-polyimides were mostly investigated in the literature experimentally by systematically varying the diamine or dianhydride ratios [9-20]. However, thousands of diamine-dianhydride combinations can be suggested as potential membrane materials, but only a limited number of them are synthesized and characterized for gas separation. At this point, group contribution methods may come in handy as a predictive tool for a quick screening of a large number of co-polyimide structures. They offer an opportunity to predict the structure-property relationship without wasting time and money in the case of failure.

A vast amount of polymer permeability data is available in the literature which allow for the development of group contribution methods to predict numerous properties such as glass transition temperature, melting point, cohesion energy, heat capacity, etc. [21, 22], and transport properties such as diffusivity, solubility and permeability [23-27] in polymers. Salame [23] was the first to use the group contribution method to predict the permeability coefficients of polymers based on cohesive energy density and FFV assigning parameter values based on the polymer repeat units. Later on, Park and Paul applied the group contribution method to predict permeability coefficients of aromatic polymers [24]. The empirical factors for 41 different structural units were determined from a permeability database of 102 polymers. Another method is the group contribution method of Alentiev et al. [25] developed specifically to predict the permeability coefficients of polyimides

using a database including about 120 polyimides prepared from 9 dianhydrides and 70 diamines. A different approach was adapted by Meares [26] who used predicted activation energy from the calculation of cohesive energy times the square of the gas diameter to calculate the diffusivity and permeability coefficients of polymers. All of these methods were suggested for the membranes synthesized from a homo-polymer. Very few predictive studies for co-polymers have been reported [28-32]. Considering the structural complexity of co-polyimides and other factors in the membrane synthesis procedure (such as solvent type, post-treatment conditions, etc.) that influence the permeability values, predicting their permeation parameters is a more difficult task.

Recently, Velioglu and Tantekin-Ersolmaz [28] have modified the group contribution method of Alentiev et al. [25] and extended it to co-polyimides:

$$logP_m = \left[\left(Ratio_{dianhydride1}\right)logM_{1m} + \left(Ratio_{dianhydride2}\right)logM_{2m}\right] + logN_m + C_m \quad (1)$$

$$logP_m = logM_m + \left[\left(Ratio_{diamine1}\right)logN_{1m} + \left(Ratio_{diamine2}\right)logN_{2m}\right] + C_m \quad (2)$$

Specific increments characteristic for certain dianhydrides (M_m, M_{1m} *and* M_{2m}) and diamines (N_m, N_{1m} *and* N_{2m}), and the gas constant (C_m) for gas type m were taken from the work of Alentiev et al. (Table 1 in ref. 31). First, Velioglu and Tantekin-Ersolmaz [28] used this new model and the database of Alentiev et al. [25] to predict the permeability coefficients of 31 different co-polyimide structures of which experimental permeability data were reported in the literature. The permeability predictions of these co-polyimides calculated from equations 1 and 2 exhibited small deviations from the experimental data. After the new model is verified, we have predicted the permeability coefficients of H_2, O_2, He, CO_2, N_2, and CH_4 gases for over 2200 hypothetical co-polyimide structures and evaluated them for separation of commercially important gas pairs [28]. The analysis of these predictions for CO_2/CH_4 separation is the basis of our current work.

We have predicted hypothetical co-polyimide structures with one dianhydride and two different diamines, and two different dianhydrides and one diamine in three different diamine-1/diamine-2 and dinahydride-1/dianhydride-2 ratios respectively. Figure 1 shows ideal selectivity-permeability diagrams for the structures that gave the best CO_2/CH_4 separation performance as defined by their position on the diagram, i.e. above the 1991 upper bound line of Robeson [33]. It should be noted here that, the only polymers (excluding TR polymers [7]), reported in the literature, that exceed the 1991 upper bound and therefore within or above the 2008 upper bound line [4] are the polymers with intrinsic microporosity (PIMs) [8], three co-polyimide structures (6FDA/PMDA-TAB (1:3),

TADATO/DSDA-DDBT (1:1), 6FDA-TMPDA/DAT (1:1)), PVSH doped polyaniline, poly(diphenyl acetylene) and PTMSP. Three other co-polyimide structures (6FDA/BPDA-DDBT (1:1), 6FDA-DABA/6FpDA (1:2) and 6FDA-DABA/DAM (1:2)) reported with slightly above 1991 upper bound performance were included in the verification of Equations 1 and 2 in the study of Velioglu and Tantekin-Ersolmaz [28] and therefore was not included in Figure 1. A general observation for Figure 1 is the fact that very few co-polyimides have separation properties above the 1991 upper bound line for CO_2/CH_4 separations. The co-polyimide structures whose separation properties exceed the 1991 upper bound are 6FDA/PMDA-p-BAPS (3:1), 6FDA/BPDA-pBAPS (3:1), 6FDA/BTDA-pBAPS (3:1), 6FDA-pBAPS/mPDA (3:1), 6FDA-pBAPS/DAM (3:1), 6FDA-pBAPS/DABA (3:1), 6FDA-pDDS/mPDA (3:1), 6FDA-pDDS/DAM (3:1) and 6FDA-pDDS/DABA (3:1). A common feature of these structures is the sulfone group in one of the diamines (pBAPS and pDDS) used to build the co-polyimide repeat unit.

The primary focus of the present study is the synthesis and characterization of three of the structures identified as promising co-plyimides as CO_2/CH_4 separation membrane materials, i.e. 6FDA/BTDA-pBAPS (3:1), 6FDA-pBAPS/DABA (3:1), and 6FDA-pBAPS/mPDA (3:1). The three structures under investigation here have the highest predicted selectivity values and shown on Figure 1 as circled data points. This paper first presents an experimental study involving the synthesis and structural and thermal characterization of the identified polymers. Then, we have prepared dense membranes from each one of these co-polyimides and measured the CO_2, CH_4, O_2, and N_2 permeability coefficients to further test the predictive capability of the group contribution model we have proposed. In addition to the experimental analysis of these structures, we have also used molecular simulation techniques to identify the most preferential sorption sites in these structures in order to further gain insight into the possible plasticization nature of these co-polyimides. In contrast to experimental studies, there are a limited number of molecular simulation studies on co-polyimides most of which focus only on their structural features [34, 35]. We analyzed not only the structural properties such as glass transition temperature (T_g), FFV and its distribution, d-spacing, radius of gyration, and cohesive energy density, but also the gas sorption isotherms to understand the dynamics of polymer chains and penetrant-polymer interactions. We have also carried out experimental sorption measurements to validate the simulations.

2. Gas Transport Theory

Gas transport through dense polymeric membranes is typically described by the solution-diffusion mechanism [2] where the driving force producing movement of a permeant is the gradient in its

chemical potential which is related to gradients of pressure, temperature, concentration, and electromotive force. The process of permeation comprises of three steps: sorption of gas molecules on the feed side of the membrane, and then the diffusion across the membrane cross-section via transient gaps in the polymer matrix, and finally desorption from the other surface of the membrane. The separation performance of a membrane is usually defined by its permeability and selectivity. For a solution-diffusion membrane, permeability, *P*, is defined as the product of diffusivity, *D*, and solubility or sorption, *S*, when the downstream pressure is significantly lower than the upstream pressure:

$$P_i = D_i \times S_i \tag{3}$$

The ideal selectivity for a binary gas feed of A and B ($\alpha_{A/B}$) is defined as the ratio of pure gas permeabilities:

$$\alpha_{A/B} = \frac{P_A}{P_B} = \frac{D_A}{D_B} \cdot \frac{S_A}{S_B} = (\alpha_D \cdot \alpha_S)_{A/B} \tag{4}$$

where P_A and P_B are the permeability coefficients of gases A and B, respectively. By default, the more permeable gas is taken as A, so that selectivity is bigger than 1. The α_D and α_S represent diffusion selectivity and sorption (solubility) selectivity, respectively. Ideal sorption selectivities of CO_2/N_2, H_2/CO_2, CO_2/CH_4, and O_2/N_2 gas pairs in the co-polyimide matrices were evaluated by calculating the ratio of the estimated sorption coefficients of the relevant gases. However, actual selectivities may differ significantly from ideal values due to plasticization and competitive sorption [27]. In a binary system consisting of gases A and B with gas A as the fast permeating gas, separation factor is defined as the concentration ratio of A to B in the permeate, and X_A and X_B are the concentration of the gases A and B in the feed.

$$\alpha_{A/B} = \frac{(Y_A / Y_B)}{(X_A / X_B)} \tag{5}$$

where $(\alpha_{A/B})$ is the separation factor in a binary system, Y_A and Y_B are the concentration of the gases A and B in the permeate.

Fick's first law governs the diffusion in the absence of bulk flow and is expressed as:

$$J = - D\nabla C \tag{6}$$

where J is the diffusive flux, D is the diffusion constant and C is the concentration of the local gas penetrants. Thus at any point inside the polymer in Cartesian coordinates, diffusion of gas penetrants in one dimension is given by:

$$J_A = - D_A \frac{\partial C_A}{\partial x} \tag{7}$$

Sorption is governed by the inherent condensability of the penetrant gas molecule and fractional free volume (FFV) of the polymer. Over the past three decades, sorption of gas molecules in glassy polymers has been described by the dual-mode sorption model as shown in equation 8 [36, 37].

$$C = k_D p + \frac{C_H' bp}{1 + bp} \tag{8}$$

The first term in equation 8 is described by Henry's Law relation and the second term is defined as Langmuir sorption which is viewed as being due to the uptake into the unrelaxed volume or microvoids present in glassy polymer. Total sorption is the sum of these two effects where C is the penetrant concentration, p is the pressure, k_d is the Henry's Law constant, b is the hole affinity constant for Langmuir sorption, and C'_H is the Langmuir sorption capacity. The ratio of the penetrant concentration to pressure is defined as the sorption coefficient:

$$S = \frac{C}{p} = k_D + \frac{C_H' b}{1 + bp} \tag{9}$$

In CO_2/CH_4 membrane separation processes, it is known that CO_2 acts as a sorption induced volume swelling agent and/or plasticizer which hinders the preference of PIs as membrane material for gas separation. Plasticization is a pressure dependent phenomenon and occurs when the concentration of CO_2 in glassy polymers is high enough to cause swelling in the polymer, i.e. reduce chain alignment and increase inter-segmental mobility and FFV [38-42]. Due to the loss in size discrimination ability, permeability of CH_4 is accelerated and as a consequence there would be a significantly high selectivity decrease. Proper molecular designs for stabilizing membranes against plasticization and hence overcoming the perm-selectivity reduction should be proposed via a fundamental understanding of penetrant induced plasticization.

3. Experimental

3.1. Polymer Synthesis

Table 1 presents the physical properties of monomers which were used in the synthesis of co-polyimides, 6FDA/BTDA-pBAPS, 6FDA-pBAPS/mPDA, and 6FDA-pBAPS/DABA. Co-polyimides were synthesized using a two-step technique. In the first step, a polyamic acid was formed in a solution of DMAc via the reaction of the dianhydride and the diamine and the second step converted the polyamic acid to polyimide by using a dehydration agent (o-DCB). The water evolving during the imidization reaction formed a low boiling point azeotrope with o-DCB which was collected on the Dean-Stark trap. In order to ensure high purity of the monomers, they were sublimed under vacuum at 5-10°C below their melting points. In the polyamic acid synthesis, dianhydride and diamine monomers were added in equimolar quantities and diamine or dianhydride ratios was scaled as 3:1. This ratio was chosen based on the predictions of the group contribution method. The monomer ratio in the reaction solution was ~ 20% by weight. Polyamic acid reaction was carried out at 4°C. Three-necked round bottom flask was continuously purged with a stream of nitrogen that was maintained throughout the entire reaction. Solution was stirred 48 hours at 4°C and the reaction was monitored with Fourier Transform Infrared Spectroscopy (FTIR) (Perkin-Elmer Spectrum One) analysis between 4000 cm^{-1} and 600 cm^{-1} wavelength until no further change was observed in the characteristic peaks (aromatic NH-C at 3500 cm^{-1}, -OH (-COOH) at 2925 cm^{-1}, and C=O (-COOH) at 1680 cm^{-1}) of the polyamic acid samples taken from the reaction medium. The imidization reaction was carried out at 180°C in an oil bath. O-DCB was added in 1:3 mole ratio of DMAc. Water formed during the reaction was condensed and collected on the Dean-Stark trap. The excess o-DCB in the Dean-Stark trap was returned back into the reaction solution to maintain a constant solvent volume in the flask. The imidization reaction was also monitored by FTIR following the characteristic polyimide peaks (symmetric and asymmetric C=O peaks at 1780 cm^{-1} and 1820 cm^{-1} respectively, and C-N vibration peak around 1350-1375 cm^{-1}). After the reaction was over, the polyimide solution was cooled and precipitated in methanol. Recovered white precipitate was then filtered, washed, and dried in a vacuum oven at 150°C for 24 h.

3.2. Membrane Preparation

The formation of dense membranes was achieved by casting-evaporation technique from a 20 wt. % solution of the co-polyimide in NMP. The surface of a glass plate was thoroughly cleaned and

heated to 100°C before casting. The polymer solution was poured on the heated glass surface and cast into a film by using a film applicator and a casting knife. The initial film thickness was set to 500 μm. The evaporation was carried out in a chamber under nitrogen atmosphere until the film was formed. The glass plate with the film was then moved to an oven for further drying for 2 hours at 80°C. The membrane was then removed from the plate and left hanging in an oven to dry out the residual solvent at 80°C for one day followed by further drying under vacuum at 80°, 150°, and 210°C for one day consecutively. The average thickness of the films was determined using a digital micrometer.

3.3. Membrane Characterization

Standard characterization methods were employed to determine the thermal and structural properties of the membranes. Thermo-gravimetric analysis (TGA) measurements were carried out with a Perkin-Elmer Diamond TG/DTA. About 3 mg of sample was weighed for both film and powder co-polyimides, and heated from 50°C to 550°C at a rate of 10°C/min. TGA analysis gave information on the amount of moisture and residual solvent in the sample, and were also used as a guide for DSC measurements.

Differential scanning calorimetry (DSC) measurements were carried out on thin films and powder samples having an average mass of 10 mg using a Perkin-Elmer 4000 Series DSC. The heating cycle described below was applied under inert N_2 atmosphere, in order to prevent unforeseen side reactions. The glass transition temperature (Tg) was calculated by half-Cp extrapolation method. The following heating sequence was designed based on the TGA analysis [43]:

- heating from 50°C to a temperature 20-30°C above Tg, at a rate of 20°C/min in order to erase the sample's thermal history without inducing irreversible transitions,
- maintaining at this temperature for about 10 min in order to evaporate the residual solvent,
- cooling down to a temperature 50-60°C below the Tg, at a rate of 30°C/min in order to prepare the sample for the next heating cycle, and
- immediate re-heating to 450°C at a rate of 20°C/min to identify the glass transition properly.

Wide angle X-ray diffraction (XRD) patterns of polyimide films were obtained using PAN analytical X-Pert PRO diffractometer with a CuKα source (λ = 1.54Å). The apparatus scanned over the range of 5-60°, with a dwell time of 3s and a step size of 0.5°. The d-spacing was calculated

from Bragg's equation, $\lambda = 2dSin\theta$. The average d-spacing is determined from a polynomial curve of the data in the region of the main peak.

Polymer film densities at 23°C were measured with a Ray-Ran density gradient column filled with aqueous zinc chloride-ethanol-water solutions. Each film density was measured at least twice.

3.4. Gas Permeability Measurements

The gas permeability measurements were carried out with an in-house built constant-volume variable-pressure permeation system shown in Figure 2 [44, 45]. The permeation system comprises a permeation cell, upstream and downstream transducers, a data acquisition system, and a gas chromatograph (GC).

To measure gas permeabilities, the masked membrane film was placed into the permeation cell with an O-ring on both halves and inserted into a pressure-rise permeation apparatus. Masking allows the use of small membrane samples to reduce the exposed membrane surface area and is done using an aluminum tape with adhesive on one side [46]. In order to remove residual solvent and sorbed gases; the upstream, downstream, and the membrane were evacuated for 24 hours using a vacuum pump. After evacuation, the pressurized gas was fed to the upstream, while the change in the pressure in the calibrated downstream volume was constantly recorded. All permeation experiments were conducted at steady-state with a linear rate of pressure increase in the downstream volume. On each membrane sample, permeability measurements for each gas were repeated until the slope of the pressure-vs-time plot remained constant. After each measurement, the downstream volume was evacuated while the upstream was exposed to a pressurized gas feed. The permeability coefficient of gas *i* (O_2, N_2, CO_2, or CH_4) was calculated using Equation 10.

$$P_i = \frac{\left(m_p - m_l\right) Vl}{ART\Delta P} \tag{10}$$

where m_p is the rate of pressure increase in the downstream during permeation measurement, m_l is the rate of leak in the downstream volume which was determined prior to gas permeation, V is the volume of the downstream, l is the thickness of the membrane, A is the permeation area of the sample, R is the ideal gas constant, T is the temperature at which the measurement was taken, ΔP is the pressure difference between the upstream and the downstream. Permeation measurements for O_2

and N_2 gases were carried out at 35°C and 2 bar upstream pressure, while those for CO_2 and CH_4 gases were carried out at 35°C and 4 bar upstream pressure.

3.5. Gas Sorption Measurements

Intelligent Gravimetric Analyser (IGA) by Hiden Isochema, UK, was used for gravimetric sorption measurements of O_2, N_2, CO_2 and CH_4 gases on co-polyimide membranes. The membrane samples of about 90 mg weight were first "degassed" at 50 mbar/min rate to remove any sorbed gases. The heating rate was 1°C/min, and the "degassing" temperature was 250°C. The samples were kept at this high temperature for 2 hours to remove residual solvent and moisture, and then cooled down to the measurement temperature (35°C). The measurement sequence was carried out between 0-9 bars, with set points at 1 bar intervals. Before the sorption measurement of another gas, the whole system was decontaminated for 2 hours.

4. Molecular Modeling

Sorption simulations were carried out using the Accelrys® Materials Studio (MS) 5.5 simulation package [47]. The simulation procedure was similar to one procedure that was applied to polyimides in a previous study [48]. The COMPASS force field was adapted to model molecular interactions [49]. All-Atom model was used to represent the gas molecules. The Van der Waals interactions were calculated by pair-wise addition, with the cut-off distance being set to the half of the simulation cell length, and Ewald summation method was used to calculate the electrostatic interactions. The calculations were performed on multi-core PCs and high performance clusters.

4.1. Model Preparation

The co-polyimide structure was assumed as alternating polyimides of two dianhydrides and one diamine or one dianhydride and two diamines. 6FDA and BTDA dianhydride, pBAPS, mPDA and DABA diamine moieties shown in Figure 3 were constructed to create first the repeat unit of 6FDA-pBAPS, BTDA-pBAPS, 6FDA-mPDA and 6FDA-DABA homo-polyimides. The co-polyimide chains with appropriate dianhydride/dianhydride (3:1) and diamine/diamine (3:1) ratios were then built by connecting these repeat units with each other by using *Random Copolymer* tool and a final geometry optimization was carried out. The total number of repeat units in the co-polyimide chains varied between 60 and 80 repeat units. A cubic simulation cell with a side of 38-40 Å for each model co-polyimide matrix was constructed from a single chain using the Amorphous Cell module

of the software package. Equilibration procedure of co-polyimide was same as the one applied to polyimides in the previous study [48]. The time step in the MD simulations was adopted as 1 fs, and the temperature and pressure were controlled through Berendsen thermostat and barostat [50], respectively. Once the model co-polyimide matrices were constructed, the X-ray scattering pattern and d-spacing, radius of gyration (Rg), dihedral distribution, cohesive energy density (CED), fractional free volume (FFV) and glass transition temperature (Tg) of each co-polyimide were estimated and compared with the experimental results. Accurate estimation of these structural properties is crucial to predict separation performance of the polymeric membrane materials.

4.2. Calculation of sorption coefficients

The Sorption module of the simulation software was used to carry out the sorption simulations in co-polyimide matrices. The calculations were carried out in the Grand Canonical Monte Carlo (GCMC) ensemble at fixed temperature, volume, and chemical potential using the Metropolis Algorithm [51]. Simulation temperature and pressure values were chosen based on the experimental studies: 35ºC and 8 bar for CO_2 and CH_4; 35ºC and 2 bar for O_2 and N_2.

5. Results and Discussion

5.1. Experimental

5.1.1. Characterization of co-polyimides

The FTIR spectra for monitoring polyamic acid and polyimide formation for all three co-polyimide structures are presented in the *Supporting Information*. Figure 4 shows FTIR spectrums of the co-polyimides. The main difference between DABA and mPDA diamines is the carboxylic acid group (-COOH). Broad weak absorption of -OH vibration (3200-3500 cm^{-1}) of carboxylic acid group in DABA diamine, which is the evidence of the presence of this group in 6FDA-pBAPS/DABA co-polyimide, can be seen clearly from Figure 4(a). C-N stretching peak around 1437 cm^{-1} are almost same in all co-polyimide FTIR spectrums. However, the nearest peak around 1463 cm^{-1}, which shows the -OH in-plane deformation, shadows the C-N stretching peak in 6FDA-pBAPS/DABA. This means that the -OH in-plane deformation occurs due to H-bonding in 6FDA-pBAPS/DABA. In addition, when 6FDA-pBAPS/DABA and 6FDA-pBAPS/mPDA are compared in Figure 4(b), there is a shift in SO_2 antisymmetric stretching peak from 1371 cm^{-1} in 6FDA-pBAPS/mPDA to 1376 cm^{-1} in 6FDA-pBAPS/DABA, which may be the indication of H-bonding. H-bonding is

followed in the literature with SO_2 stretching (1324, 1147 cm^{-1}) [52], ether group (1232 cm^{-1}) [52, 53] in pBAPS diamine, broad weak absorption of -OH vibration (3200-3500 cm^{-1}) of carboxylic acid group in DABA diamine [54], and the OH in-plane deformation (1395-1440 cm^{-1}) of carboxyl dimers [55]. In addition, the presence of hydrogen bonding between structures can be determined by observing shifts of characteristic absorption bands to higher wave numbers or noting changes in peak intensities [52, 53].

The experimentally determined structural properties of co-polyimides are presented in Table 2 along with the predicted values obtained from the molecular simulation study, which are discussed in section 5.2. We will only examine the experimental results in this section. The X-ray diffraction analyses showed that the d-spacing values changed only slightly when a second diamine (mPDA) instead of a second dianhydride (BTDA) was used in the considered co-polyimides. However, the X-ray patterns of co-polyimides in Figure 5 exhibit clearly a shoulder at 2θ=~27º for 6FDA-pBAPS/mPDA, which is the indication of existence of small free volumes or free volume distribution different than 6FDA/BTDA-pBAPS [37, 56]. Among the three co-polyimides considered in this study, 6FDA-pBAPS/DABA has the highest d-spacing value due to the carboxylic acid side groups which inhibits packing due to the steric hindrance. However, 6FDA-pBAPS/DABA co-polyimide has high density and low radius of gyration (Rg) due to hydrogen bonding ability of –OH group in carboxylic acid of DABA diamine as mentioned in FTIR analysis. It enhances close packing and hence increases the cohesive energy of co-polyimide. When 6FDA-pBAPS/DABA and 6FDA-pBAPS/mPDA are compared, this relation becomes obvious. However, it is expected that 6FDA-pBAPS/DABA should have low FFV and d-spacing compared to the 6FDA-pBAPS/mPDA. In the next section, it will be clearly presented that with the addition of –OH groups, hydrogen bonding increases Langmuir sorption sites and decreases Henry sorption sites. Due to the increase in Langmuir sorption sites, the un-relaxed “frozen” excessive free volume present in 6FDA-pBAPS/DABA co-polyimide increased slightly.

The DSC measurements show that the Tg values of all three co-polyimides are close to each other (Table 2). The reported Tg values of films prepared from the corresponding homo-polyimides in the literature in Table 3 reflect a variation due to the presence of a variety of effects in film preparation. The measured Tg values of the co-polyimides are within the lowest and highest of their corresponding homo-polyimides.

Thermogravimetric analysis of membranes is applied in order to determine the amount of sorbed moisture and residual solvent present within the membrane. Figure 6 shows the TGA thermograms

for co-polyimide membranes where Table S1 (in *Supporting Information*) lists the mass loss for these samples. All co-polyimides have nearly same degradation temperature. However, 6FDA-pBAPS/DABA co-polyimide has a minor weight loss at about 300ºC, prior to major backbone degradation at about 500ºC, which can be seen as a small peak in the derivative weight curve of Figure 6. Similar thermal degradation behavior was reported in the literature [12, 54, 55, 66, 67] for polymers which have DABA diamine monomer in the polymer backbone; the characteristic small peak in the weight derivative curve at around 300-370ºC is attributed to decarboxylation of -COOH moieties. When the TGA curves of the 6FDA-pBAPS/mPDA and 6FDA-pBAPS/DABA in our work are compared, it can be observed that the main difference between these co-polyimides is the carboxylic acid group in the second diamine. We can conclude that these carboxylic acid groups (-COOH) form weak hydrogen bonds and hence increase the polymer packing and reduce free volume between polymer chains in line with the reports in literature. One-step degradation curves are obtained for all co-polyimides under study here except 6FDA-pBAPS/DABA. TGA curves show that 6FDA/BTDA-pBAPS and 6FDA-pBAPS/mPDA possesses good thermal stability with no significant weight loss up to temperatures of approximately 480ºC in nitrogen atmosphere. In addition, the temperatures at 10% weight loss, which are often used as the criterion of the thermal stability for high temperature polymers are all higher than 500ºC for all co-polyimides. Moreover, all of the co-polyimides maintain higher than 80% of their original weight at 550ºC.

5.1.2. Gas permeation measurements

Table 4 shows the experimental permeabilities and selectivities for co-polyimide membranes annealed at 210°C (below Tg) and the predicted permeabilities and selectivities by the group contribution method at 35ºC and 10 bar. Experimental permeabilities of 6FDA/BTDA-pBAPS membrane for all gases exhibit smaller values compared to 6FDA-pBAPS/mPDA where similar tendency was observed in the group contribution method (GCM). Comparatively higher permeability values of 6FDA-pBAPS/mPDA may be associated due to the presence of smaller d-spacing at around 3.4 Å which can be seen as a shoulder in the X-ray pattern in Figure 5. The extra small d-spacing values may be attributed to the structural difference of mPDA, a globular molecule, and pBAPS, a linear and longer molecule. During packing, the presence of mPDA may create extra small free volumes where CO_2 can permeate through but other gases which have kinetic diameters larger than CO_2 cannot permeate. This hypothesis can be somewhat quantified by looking at the X-ray analysis. The d-spacing value calculated for the shoulder at 2θ =~27º in Figure 5 is calculated to be 3.4 Å, larger than CO_2 kinetic diameter and smaller than that of methane and nitrogen. It must be noted that, although the ratio of this small peak to the main peak in the X-ray pattern of the co-

polyimide is very small, the effect it has on the CO_2 permeability of the resultant membrane is rather significant. This effect has even bigger impact on CO_2/CH_4 and CO_2/N_2 selectivities.

When 6FDA-pBAPS/mPDA and 6FDA-pBAPS/DABA transport properties are compared, it can be seen that, by changing mPDA with DABA as the second diamine, the permeabilities of all gases drop down, while the selectivities are increasing. The DABA monomer contains a polar carboxylic acid group whereas mPDA does not contain any side groups at all. Yampolskii suggested in his review paper that the introduction of the substituents that are capable of making dipole−dipole interactions can form hydrogen bonds and strongly influence the transport parameters due to increasing inter-chain interactions or interactions with some penetrants [68]. Plate and Yampolskii reported that when the content of −COOH groups in polymer matrix increased to 20%, a significant decrease in permeability values of polar diffusants were obtained [69]. Hirayama et al. [61] also observed similarly a decrease in permeability of O_2 from 3 to 1 Barrer with an increase in separation factor of O_2/N_2, when they replaced the mPDA diamine with DABA.

In 1991, Robeson [33] defined a so-called upper-bound, which represents the upper limit for the performance of polymeric membranes and revised it in 2008 [4]. Figure 7 shows the upper-bound for CO_2/CH_4, O_2/N_2, and CO_2/N_2 gas pairs, in the plots of selectivity versus permeability of faster-permeating gas. Predictions of group contribution method for all gases in three co-polyimides generally overestimate the measured permeability coefficients. However, these co-polyimides still remain in the commercially attractive region for the CO_2/CH_4 gas pair but under 2008 upper bound line [4]. The differences between GCM predictions and experimental values are not surprising considering the assumptions involved in the GCM and the experimental variations due to the factors such as polymer synthesis conditions, film formation procedure, solvent type, annealing conditions, etc. which all influence the permeability values due to their effect on the conformation of the polymer chain. In spite of all the simplifications and assumptions involved in group contribution method and the structural complexity of co-polyimides, the agreement between the predicted and experimental values clearly shows that GCM can be used for identifying possible co-polyimide structures to lead experimental studies.

Apart from tailoring the separation properties of two homo-polyimides by combining them with a defined ratio, co-polyimides may also give an opportunity to synthesize plasticization resistant, robust membrane materials with the judicious selection of the monomers. Plasticization is a serious concern limiting the use of PIs as membrane material for gas separation involving CO_2, H_2S and condensable hydrocarbons. In order to see the plasticization behavior of these co-polyimides in the

presence of CO_2, permeation experiments are only performed up to ~9 bar due to the limitations of the permeability system in our laboratory. Figure 8 shows that all three co-polyimides do not show any significant sign of plasticization up to ~9 bars.

5.1.3. Gas sorption measurements

Table 5 shows the sorption coefficients of CO_2, CH_4, O_2, and N_2 gases obtained from IGA measurements. This table also shows the data obtained from the molecular simulation studies which will be discussed in section 5.2.3. The sorption coefficients and selectivities of these light gases in all co-polyimides are close to each other indicating that they are diffusion selective like most polyimides. There is a slight decrease in CO_2 and CH_4 sorption selectivities of 6FDA/BTDA-pBAPS compared to 6FDA-pBAPS/mPDA co-polyimide possibly due to the difference in the pBAPS content of these co-polyimides. The 6FDA/BTDA-pBAPS contains 50 mole % pBAPS whereas pBAPS mole ratio is 37.5% in 6FDA-pBAPS/mPDA. A qualitative relationship between the concentration of polar moieties in the polymer and gas sorption selectivity can be found in the literature [70, 71]. Koros suggested that CO_2/CH_4 sorption selectivity increases with the concentration of carbonyl or sulfonyl groups in the polymer backbone [70]. A similar conclusion was drawn by Bondar et al. [71] stating that the increase in the mass density of ether linkages or carbonyl groups leads to higher sorption selectivity. Hence, the slightly higher sorption selectivity of 6FDA/BTDA-pBAPS compared to 6FDA-pBAPS/mPDA may be due to the high mass density of ether linkages and sulfonyl group in pBAPS diamine. However, this finding cannot be used to explain the sorption differences between 6FDA-pBAPS/mPDA and 6FDA-pBAPS/DABA since they contain the same concentration of pBAPS diamine. In this case, the decrease in all gas sorption measurements of 6FDA-pBAPS/DABA may be attributed to the carboxylic acid group in the DABA diamine. The carboxylic acid group in the DABA diamine forms hydrogen bonds with sulfonyl and carbonyl groups and therefore does not interact with CO_2. Lin and Freeman [72] show in their work with polymers containing polar groups (copolymers of butadiene and acrylonitrile, polymers containing carbonate groups, polybutadiene, poly(tetramethylene oxide), poly(ethylene oxide), and poly(vinyl acetate)) that hydrogen bonding increases the solubility parameter, thereby decreasing CO_2 solubility; this is in line with the observation in this work.

Table 6 shows the dual mode sorption constants of CO_2 for all co-polyimides at 35°C, in which 6FDA-pBAPS/mPDA co-polyimide has the highest Henry's law constant and lowest Langmuir parameter. Due to its high Henry's law constant (Eq. 2), 6FDA-pBAPS/mPDA co-polyimide shows slightly higher CO_2 sorption coefficients for the pressure range investigated here. Dong et al. states

that in most cases, Langmuir sites adsorb a much smaller quantity of gas penetrant than Henry's sites considering that the differences in surface area available in these two sites differ by several orders of magnitude [73]. This conclusion is consistent with our findings. Moreover, k_D and b are related to the enthalpy of dissolution (ΔH_D) and the apparent enthalpy of hole-filling respectively, which are dependent on the nature of polymer–penetrant interaction [74]. As a result, the strongest co-polyimide–penetrant interactions can be observed from the highest values of k_D and b, in our case obtained for 6FDA-pBAPS/mPDA.

It is known that CO_2 concentration depends strongly on the FFV of polymers at the considered pressure. CO_2 sorption capacities of co-polyimides can be seen from sorption isotherm in Figure 9. No great differences in gas uptakes are noticed between the three co-polyimides. As will be seen later in section 5.2, molecular simulation results predicted no considerable difference in the FFV values of these polymers.

5.2. Molecular Modeling

5.2.1. Characterization of co-polyimides

In order to verify the accuracy of a simulated polymer model, the structural properties of the polymer are usually calculated from molecular simulations and compared to the experimentally measured values. Table 2 presents the structural properties of the three co-polyimide models in comparison to experimental results. Calculated d-spacing, density, and Tg values agree well with the experimental values. The agreement between experimental and predicted values is a strong indication of the accuracy of the polymer models built for simulation studies.

5.2.2. Fractional Accessible Volume (FAV)

The analysis of the volume distribution by calculating the Fractional Accessible Volume (FAV) instead of free volume is a more useful approach to measure conformational changes in the polymer chains [75, 76]. The FAV is estimated from the *Connolly* task simulation by using different probe diameters to detect the available vacancy inside the simulation unit cell. Figure 10 compares FAV distribution as a function of probe size for the three co-polyimides. The FFV volumes of co-polyimides are almost same (Table 2) and there are no significant differences in their FAV distribution for probe sizes 0.0-1.6 as seen in Figure 10. However, at probe sizes of 1.6-2.0 and 2.0-2.4 Å corresponding to the kinetic diameter of a CO_2 molecule (i.e. CO_2 can be adsorbed), there is a

slight increase in FAV percentage of 6FDA-pBAPS/mPDA compared to the other co-polyimides which means that 6FDA-pBAPS/mPDA has a slightly larger free volume that enhance sorption. This also indicates that it has larger FFV surface area which may increase available sorption sites. This observation in free volume distribution is supported by the x-ray analysis presented in Figure 5 where a shoulder is observed in the X-ray of 6FDA-pBAPS/mPDA around a 2θ values of 27º.

5.2.3. Sorption simulations

The results of the GCMC simulations to estimate the sorption of CO_2, CH_4, O_2, and N_2 gases in the model co-polyimide matrices are presented in Table 5. The predicted sorption coefficients of these light gases in all co-polyimides are generally in good agreement with the experimental data obtained by IGA. In addition to single gas calculations, binary gas sorption simulations for light gases are carried out. In binary gas separation processes, both gases are in the same flow and in contact with each other. It is generally difficult to measure the ideal sorption selectivity, which is calculated by taking the ratio of pure gas sorption coefficients. However, ideal and binary selectivities may differ significantly due to the combined effects of the competition between the penetrants, gas phase non-ideality, plasticization phenomena, and gas polarization. Table 7 compares the simulated ideal (pure gas) and binary (50:50 mixture) sorption selectivities of the three co-polyimides for CO_2 and CH_4 at 35°C and 10 bar. The binary gas sorption results suggest that there are gas-gas and gas-polymer interaction effects which drastically alter the transport properties of CO_2 and CH_4. The comparison between mixed gas and single gas solubility coefficients for both gases clearly reveals that the competition for the available sorption sites favors CO_2 resulting in much higher sorption selectivities. The CO_2/CH_4 sorption selectivity of 6FDA/BTDA-pBAPS increases more than 9-fold whereas the increase is approximately 6-fold and 4-fold for 6FDA-pBAPS/mPDA and 6FDA-pBAPS/DABA, respectively. This indicates that the interaction of CO_2 with 6FDA/BTDA-pBAPS is higher due to the higher amount of pBAPS monomer as discussed above. Also, the presence of DABA structure, which enhances hydrogen bonding, lowers the CO_2 adsorption.

5.2.4. Radial distribution functions (RDF)

RDFs can be used for an in-depth analysis of atomic interactions between penetrants and the co-polyimide matrices. Based on the location and intensity of the peaks in the RDF, one can determine the preferential sorption sites on the polymer chain for a particular sorbate. Figure 11 presents the RDFs of CO_2 (with 47, 55 and 60 CO_2 molecules which correspond to the equilibrium

concentrations at 8 bar and 35°C in 6FDA/BTDA-pBAPS, 6FDA-pBAPS/mPDA and 6FDA-pBAPS/DABA respectively) around seven typical atoms of repeat units in co-polyimide chains: (1) the oxygen and (2) nitrogen in the imide, (3) the fluorine in the -CF_3 group, (4) the oxygen in the ether linkage, (5) sulfone in the sulfonyl linkage, (6) carbon in the –CO– group of BTDA monomer and (7) single bonded oxygen of carboxylic acid (labeled as O1, N1, F, O2, S, C, and O3 respectively). As seen in Figure 11, the sulfone group (S) in pBAPS diamine is the preferential sorption site in all three co-polyimides, but its affinity to CO_2 is the highest in 6FDA/BTDA-pBAPS and the lowest in 6FDA-pBAPS/DABA. This result agrees well with a prior simulation study by Lyulin et al. [77], who showed that the presence of the sulfone group in a BAPS containing polyimide (R-BAPS) leads to a substantial dipole moment which cannot be neglected. A similar effect may be the cause of higher CO_2 affinity in our work.

The N and O1 sites are also the preferential sorption sites for CO_2 for all three co-polyimides. 6FDA-pBAPS/DABA includes an extra sorption site of O3 in the DABA diamine which is not the most preferential sorption site for CO_2. Due to the rigid structure of 6FDA-pBAPS/DABA arisen from H-bonding between the carboxylic acid and sulfone groups (as demonstrated by FTIR analysis in section 5.1.1), it has a more closed packed structure compared to the other co-polyimides and hence low sorption capacity. This can be seen by comparing the RDFs of CO_2 in 6FDA-pBAPS/mPDA and 6FDA-pBAPS/DABA. When the diamine moiety was changed from mPDA to DABA, the intensity of the peak for the interaction of CO_2 molecules with the oxygen (O1) in the imide increased. This means that, after the sulfone groups are fully saturated, the CO_2 molecules prefer to go to the second preferential sorption site which is O1, and therefore the sorption capacity of 6FDA-pBAPS/DABA should enhance. However, the more closed packed structure of 6FDA-pBAPS/DABA and its lower free volume hinder CO_2 sorption as clearly indicated by the single gas sorption data in Table 5.

Two different speculations can be propounded from RDF analysis with regard to plasticization. First, all these sulfone containing co-polyimides which show high selectivity values display significant interactions with CO_2 and the main location of the interaction is the sulfone group (i.e. it is the most preferential sorption site). However, this CO_2–polymer interaction may also cause sorption-induced plasticization in the backbone of the polymer structure. When the most preferential sorption site is in the backbone, the effect of the plasticization is expected to be more detrimental. In order to avoid a major selectivity reduction due to plasticization without sacrificing much from the high CO_2 sorption, these sulfone groups can be attached to the side groups of diamines instead of the backbone. Tanaka et al. [78] attached sulfonated side groups to the diamine

of 2,2-bis[4-(4-aminophenoxy)phenyl] hexafluoro propane and investigated the separation performance of polyimides with and without the sulfonated groups. They reported that the sulfonated polyimide displayed high CO_2/CH_4 selectivity compared to its precursor due to the increase in sorption selectivities. However, they have not analyzed the plasticization behavior of these polyimides. In fact, there is not any study in the literature which compares the plasticization resistance of sulfonated and non-sulfonated polyimides. Second, the carboxylic acid group in the DABA diamine does not show any significant interaction with CO_2 indicating resistance to plasticization relatively. The carboxylic acid group displays H-bonding with the sulfone group of the BAPS diamine and oxygen in the imide linkage, hence results in a more closed packed structure and reduction in permeability. Therefore, if the DABA diamine is used with a diamine with high fractional free volume, it may be possible to benefit from its ability to make H-bonding and cross-link without sacrificing from permeability. For example, Kratochvil and Koros [54], and Qiu et al. [55], and Askari and Chung [79], used DABA with DAM and Durene diamines, respectively, due to their capability of increasing FFV.

6. Conclusions

The three co-polyimide structures (6FDA/BTDA-pBAPS, 6FDA-pBAPS/mPDA and 6FDA-pBAPS/DABA) identified as the promising membrane polymers for CO_2/CH_4 separation by the Group Contribution Method of Alentiev et al. [25] (modified for co-polyimides [28]) are successfully synthesized. The molecular weight of the co-polyimides varied between 50 and 100 kDa. The TGA analysis of the co-polyimides showed that 6FDA/BTDA-pBAPS and 6FDA-pBAPS/mPDA are stable up to a degradation temperature of higher than 500ºC. However, two-step degradation curve is observed for 6FDA-pBAPS/DABA. The glass transition temperatures and densities of the co-polyimides are within 276-287 ºC and 1.387-1.419 g/cm^3 range, respectively. The d-spacing value of 6FDA-pBAPS/DABA is the highest within the three co-polyimides investigated here.

Hydrogen bonding ability of the carboxylic acid groups in the DABA diamine is determined by observing the shifts in the characteristic absorption bands in the FTIR spectra and the minor weight loss before the degradation of polymer in the TGA thermogram. The formation of hydrogen bonds reduces the free volume between polymer chains by keeping them in the minimum interstitial distances. This hydrogen bonding also restrains the polymer chain from free rotation and mobility leading to a possible inhibition of sorption-induced plasticization.

The O_2, N_2, CO_2 and CH_4 permeability coefficients for the co-polyimides measured by constant-volume-variable pressure method at 35°C are in good agreement with the values estimated by the Group Contribution Method [28]. This is rather remarkable considering all the simplifications and assumptions involved in the group contribution method. The predictive power of group contribution methods is closely related to the number and accuracy of the data used in the analysis. The Group Contribution Method used in our previous study, results of which are the motivation of this work, utilizes a large database of permeability values for polyimides and therefore its statistical significance should not be underestimated. The agreement between the predicted and experimental values we have seen here suggests that group contribution methods can be used as a simple tool to lead experimental studies.

Experimental permeabilities of 6FDA-pBAPS/mPDA for all gases are the highest while all selectivities are the lowest within the three co-polyimides investigated here. However, 6FDA/BTDA-pBAPS has the highest experimental and predicted CO_2/CH_4 (51.9 and 126), and CO_2/N_2 (28.6 and 48.5) selectivities. Experimental permeability coefficients for all gases in three co-polyimides are under 1991 upper bound, however these co-polyimides remain in the commercially attractive region for the CO_2/CH_4 gas pair. Predicted and measured CO_2/N_2 separation performance of the co-polyimide structures are all below the 2008 upper bound. Comparatively high CO_2 permeability coefficient is determined in 6FDA-mPDA/pBAPS probably owing to the presence of small d-spacing at around 3.4 in X-ray pattern. On the other hand, due to the revealed H-bonding effect by FTIR analysis in carboxylic acid group of DABA diamine, nearly half of the permeability coefficients in all gases are gained in 6FDA-pBAPS/DABA compared to the 6FDA-pBAPS/mPDA. This difference is not detected in sorption measurements which mean that it is arisen from the differences in gas diffusion. The CO_2 plasticization behavior of these co-polyimides is investigated experimentally and the plasticization effect is not observed up to 9 atm.

Molecular simulation methods are used for construction of co-polyimide structures. The structural properties of the investigated polymers are estimated in good agreement with the experimental data, which indicates that molecular simulation can be used successfully to characterize various polyimide structures. Simulation of the sorption process of CO_2 is successfully reproduced in all polymers. Simulated and measured sorption coefficient well match with each other in each co-polyimide. According to the dual mode sorption calculations achieved from experimental gravimetric measurements, the contribution of the Henry solubility coefficients to the total CO_2 solubility is significant for 6FDA-pBAPS/mPDA membrane. The presence of higher free volume between adjacent polymer chains in 6FDA-pBAPS/mPDA than other co-polyimides, which is

clearly seen by the standard model of Henry's law dissolution, is supported by X-ray analysis with the second peak seen as a shoulder corresponds to small pores.

RDFs revealed the penetrant-polymer interactions responsible for the increase in sorption coefficients. Considering the defined sorption sites in three co-polyimides, sulfone group (S) in pBAPS diamine arises as the most preferential sorption site in this study, but its affinity to CO_2 is highest in 6FDA/BTDA-pBAPS and lowest in 6FDA-pBAPS/DABA. This difference may be due to the presence of carboxylic acid groups in DABA diamine which makes H-bonding. Moreover, CO_2 is also preferentially found in the vicinity of side groups on the co-polyimide like the carbonyl oxygen (O1). Further studies on the CO_2 plasticization of these co-polyimides at high pressures are in progress and will be addressed in a subsequent paper.

Abbreviations:

6FDA: 4,4-hexafluoro isopropylidene diphthalicanhydride

BTDA: 3,3-4,4-benzophenone tetracarboxyclic dianhydride

pBAPS: bis [4-(4-aminophenoxy) phenyl] sulfone

mPDA: 1,3-phenylenediamine

DABA: 3,5-diamino benzoic acid

PMDA: pyromellitic dianhydride

TAB: 3,3',4,4'-tetraminobiphenyl

TADATO: Thianthrene - 2,3,7,8 - tetracarboxylic dianhydride - 5,5,10,10 - tetraoxide

DSDA: 4,4',5,5'-sulfonyldiphthalic anhydride

DDBT: 3,7-diamino-2,8(6)-dimethyldibenzothiophene sulfone

TMPDA: 2,3,5,6-tetramethyl-1,4-phenylenediamine

DAT: 2,6-diamine toluene

PVSH: poly-(vinylsulfonic acid)

PTMSP: poly[1-(trimethylsilyl)-1-propyne]

BPDA: 3,3′,4,4′-biphenyltetracarboxylic dianhydride

6FpDA: 4,4'- (hexafluoroisopropylidene) dianiline

pDDS: 4,4'-diaminodiphenylsulfone

R-BAPS: 1,3-bis(3′,4-dicarboxyphenoxy)benzene(dianhydirde)-4,4′-bis(4″-aminophenoxy)biphenyl sulfone)(diamine)

Durene: 2,3,5,6-tetramethyl-1,4-phenylenediamine

Acknowledgement

This work is partially supported by the Scientific and Technological Research Council of Turkey (TUBITAK) through Grant No. 106M339.

REFERENCES

[1] Y. Yampolskii, I. Pinnau, B. Freeman, Material science of membranes for gas and vapor separation, John Wiley & Sons, Ltd, England, 2006.

[2] R. W. Baker, Membrane technology and applications, John Wiley & Sons, Ltd, Menlo Park, California, 2004.

[3] A. K. Pabby, S. S. H. Rizvi, A. M. S. Requena. Handbook of Membrane Separations: Chemical, Pharmaceutical, Food, and Biotechnological Applications, CRC Press, Taylor & Francis Group, United States of America, 2008.

[4] L. M. Robeson, The upper bound revisited, Journal of Membrane Science 320 (2008) 390-400.

[5] R. R. Tiwari, Z. P. Smith, H. Lin, B. D. Freeman, D. R. Paul, Gas permeation in thin films of “high free-volume” glassy perfluoropolymers: Part II. CO2 plasticization and sorption, Polymer 61 (2015) 1–14.

[6] W. F. Yong, K. H. A. Kwek, K. S. Liao, T. S. Chung, Suppression of aging and plasticization in highly permeable polymers, Polymer 77 (2015) 377–386.

[7] H. B. Park, C. H. Jung, Y. M. Lee, A. J. Hill, S. J. Pas, S. T. Mudie, E. Van Wagner, B. D. Freeman, D. J. Cookson, Polymers with cavities tuned for fast selective transport of small molecules and ions, Science 318 (2007) 254-258.

[8] P. M. Budd, K. J. Msayib, C. E. Tattershall, B. S. Ghanem, K. J. Reynolds, N. B. McKeown, D. Fritsch, Gas separation membranes from polymers with intrinsic microporosity, Journal of Membrane Science 251 (2005) 263.

[9] X.Y. Chen, S. Kaliaguine, Mixed gas and pure gas transport properties of copolyimide membranes, Journal of Applied Polymer Science 128 (2013) 380-389.

[10] Y. Li, M. Ding, J. Xu, Gas permeation properties of copolyimides from 1,4-bis(3,4-dicarboxyphenoxy) benzene dianhydride and 2,2-bis(3,4-dicarboxyphenyl) hexafluoroisopropane dianhydride, Polymer International 42 (1997) 121-126.

[11] E. M. Maya, A. E. Lozano, J. de Abajo, J.G. de la Campa, Chemical modification of copolyimides with bulky pendent groups: Effect of modification on solubility and thermal stability, Polymer Degradation and Stability 92 (2007) 2294-2299.

[12] E. M. Maya, A. Tena, J. de Abajo, J.G. de la Campa, A.E. Lozano, Partially pyrolyzed membranes (PPMs) derived from copolyimides having carboxylic acid groups. Preparation and gas transport properties, Journal of Membrane Science 349 (2010) 385–392.

[13] M. Mikawa, S. Nagaoka, H. Kawakami, Gas transport properties and molecular motions of 6FDA copolyimides, Journal of Membrane Science 163 (1999) 167–176.

[14] M. Niwa, S. Nagaoka, H. Kawakami, Preparation of novel fluorinated block copolyimide membranes for gas separation, Journal of Applied Polymer Science 100 (2006) 2436–2442.

[15] L. Wang, Y. Cao, M. Zhou, Q. Liu, X. Ding, Q. Yuan, Gas transport properties of 6FDA-TMPDA/MOCA copolyimides, European Polymer Journal 44 (2008) 225–232.

[16] F. Piroux, E. Espuche, R. Mercier, M. Pineri, Sulfonated copolyimides: influence of structural parameters on gas separation properties, Desalination 145 (2002) 371-374.

[17] W. H. Lin, R. H. Vora, T. S. Chung, Gas transport properties of 6FDA-Durene/1,4- phenylenediamine (pPDA) copolyimides, Journal of Polymer Science: Part B: Polymer Physics 38 (2000) 2703–2713.

[18] H. Inoue, Y. Sasaki, T. Ogawa, Properties of copolyimides prepared from different tetracarboxylic dianhydrides and diamines, Journal of Applied Polymer Science 62 (1996) 2303-2310.

[19] L. Wang, Y. Cao, M. Zhou, X. Qiu, Q. Yuan, Synthesis, characterization, and gas permeation properties of 6FDA-2,6-DAT/mPDA copolyimides, Frontiers of Chemistry in China 4(2) (2009) 215–221.

[20] S. L. Liu, R. Wang, T. S. Chung, M. L. Chng, Y. Liu, R. H. Vora, Effect of diamine composition on the gas transport properties in 6FDA-durene/3,3'-diaminodiphenyl sulfone copolyimides, Journal of Membrane Science 202 (2002) 165–176.

[21] G. Bogdanic, Group contribution methods for estimating the properties of polymer systems, Hemijska Industrija 60 (2006) 287-305.

[22] D. W. Van Krevelen, Properties of polymers, Elsevier, The Netherlands, 3rd Ed. 1990.

[23] M. Salame, Prediction of gas barrier properties of high polymers, Polymer Engineering and Science 26 (1986) 1543-1546.

[24] J. Y. Park, D. R. Paul, Correlation and prediction of gas permeability in glassy polymer membrane materials via a modified free volume based group contribution method, Journal of Membrane Science 125 (1997) 23-39.

[25] A. Y. Alentiev, K. A. Loza, Y. P. Yampolskii, Development of the methods for prediction of gas permeation parameters of glassy polymers: polyimides as alternating co-polymers, Journal of Membrane Science 167 (2000) 91–106.

[26] P. Meares, The diffusion of gases through polyvinyl acetate, Journal of the American Chemical Society 76 (1954) 3415-3422.

[27] Y. Hirayama, T. Yoshinaga, Y. Kusuki, K. Ninomiya, T. Sakakibara, T. Tamari, Relation of gas permeability with structure of aromatic polyimides I, Journal of Membrane Science 111 (1996) 169-182.

[28] S. Velioğlu, S. B. Tantekin-Ersolmaz, Prediction of gas permeability coefficients of copolyimides by group contribution methods, Journal of Membrane Science 480 (2015) 47–63.

[29] A. E. Barnabeo, W. S. Creasy, L. M. Robeson, Gas permeability characteristics of nitrile-containing block and random copolymers, Journal of Polymer Science: Polymer Chemistry Edition 13 (1975) 1979–1986.

[30] L. M. Robeson, C. D. Smith, M. Langsam, A group contribution approach to predict permeability and permselectivity of aromatic polymers, Journal of Membrane Science 132 (1997) 33.

[31] J. C. Maxwell (1873) Treatise on electricity and magnetism, vol. I Oxford University Press, London.

[32] V. Ryzhikh, D. Tsarev, A. Alentiev, Yu. Yampolskii, A novel method for predictions of the gas permeation parameters of polymers on the basis of their chemical structure, Journal of Membrane Science 487 (2015) 189-198.

[33] L. M. Robeson, Correlation of separation factor versus permeability for polymeric membranes, Journal of Membrane Science 62 (1991) 165-185.

[34] E. Pinel, D. Brown, C. Bas, R. Mercier, N. D. Alberola, S. Neyertz, Chemical influence of the dianhydride and the diamine structure on a series of copolyimides studied by molecular dynamics simulations, Macromolecules 35 (2002) 10198-10209.

[35] I. Tanis, D. Brown, S. J. Neyertz, R. Heck, R. Mercier, A comparison of homopolymer and block copolymer structure in 6FDA-based polyimides, Physical Chemistry Chemical Physics 16 (2014) 23044-23055.

[36] W. R. Vieth, K. J. Sladek, A model for diffusion in a glassy polymer, Journal of Colloid Science 20 (1965) 1014-1033.

[37] R. L. Burns, W. J. Koros, Structure property relationships for poly(pyrrolone-imide) gas separation membranes, Macromolecules 36 (2003) 2374-2381.

[38] J. D. Wind, S. M. Sirard, D. R. Paul, P. F. Green, K. P. Johnston, W. J. Koros, Relaxation dynamics of CO_2 diffusion, sorption, and polymer swelling for plasticized polyimide membranes, Macromolecules 36 (2003) 6442-6448.

[39] A. Bos, I. Punt, H. Strathmann, M. Wessling, Suppression of gas separation membrane plasticization by homogeneous polymer blending, AIChE Journal 47 (2001) 1088-1093.

[40] J. S. Lee, W. Madden, W. J. Koros, Antiplasticization and plasticization of Matrimid® asymmetric hollow fiber membranes. Part B. Modeling, Journal of Membrane Science 350 (2010) 242–251.

[41] A. F. Ismail, W. Lorna, Penetrant-induced plasticization phenomenon in glassy polymers for gas separation membrane, Separation and Purification Technology 27 (2002) 173–194.

[42] D. F. Sanders, Z. P. Smith, R. Guo, L. M. Robeson, J. E. McGrath, D. R. Paul, B. D. Freeman, Energy-efficient polymeric gas separation membranes for a sustainable future: A review, Polymer 54 (2013) 4729-4761.

[43] J. D. Menczel, R. B. Prime, Thermal analysis of polymers, Wiley, 2009.

[44] A. Kilic, C. Atalay-Oral, A. Sirkecioglu, S. B. Tantekin-Ersolmaz, M. G. Ahunbay, Sod-ZMOF/Matrimids mixed matrix membranes for CO_2 separation, Journal of Membrane Science 489 (2015) 81–89.

[45] A. Kertik, Gas purification using polymer/zeolite composite membranes, M.Sc. Thesis, Istanbul Technical University, 2010.

[46] T. T. Moore, S. Damle, P. J. Williams, W. J. Koros, Characterization of low permeability gas separation membranes and barrier materials; design and operation considerations, Journal of Membrane Science 245 (2004) 227–231.

[47] Materials studio 5.0 edition. San Diego: Accelrys; 2009.

[48] S. Velioğlu, M. G. Ahunbay, S. B. Tantekin-Ersolmaz, Investigation of CO_2-induced plasticization in fluorinated polyimide membranes via molecular simulation, Journal of Membrane Science 417 (2012) 217-227.

[49] Polymer User Guide, Amorphous Cell Section, Version 4.1; Molecular Simulations: San Diego, 2000.

[50] H. J. C. Berendsen, J. P. M. Postma, W. F. van Gunsteren, A. DiNola, J. R. Haak, Molecular dynamics with coupling to an external bath, Journal of Chemical Physics 81 (1984) 3678-3683.

[51] D. Frenkel, B. Smith, Understanding molecular simulation: from algorithms to applications, Academic Press, 2002.

[52] B. D. Reid, F. A. Ruiz-Trevino, I. H. Musselman, K. J. Jr. Balkus, J. P. Ferraris, Gas permeability properties of polysulfone membranes containing the mesoporous molecular sieve MCM-41, Chemical Material 13 (2001) 2366-2373.

[53] B. Zornoza, S. Irusta, C. Tellez, J. Coronas, Mesoporous silica sphere-polysulfone mixed matrix membranes for gas separation, Langmuir 25 (10) (2009) 5903–5909.

[54] A. M. Kratochvil, W. J. Koros, Decarboxylation-induced cross-linking of a polyimide for enhanced CO_2 plasticization resistance, Macromolecules 41 (2008) 7920-7927.

[55] W. Qiu, C. C. Chen, L. Xu, L. Cui, D. R. Paul, W. J. Koros, Sub-Tg cross-linking of a polyimide membrane for enhanced CO_2 plasticization resistance for natural gas separation, Macromolecules 44 (2011) 6046–6056.

[56] V. P. Shantarovich, I. B. Kevdina, Yu. P. Yampolskii, A. Yu. Alentiev, Positron Annihilation Lifetime Study of High and Low Free Volume Glassy Polymers: Effects of Free Volume Sizes on the Permeability and Permselectivity, Macromolecules 33 (20) (2000) 7453–7466.

[57] P. S. G. Krishnana, R. H. Vora, S. Veeramania, S. H. Goh, T. S. Chung, Kinetics of thermal degradation of 6FDA based copolyimides - I, Polymer Degradation and Stability 75 (2002) 273–285.

[58] L. Cui, W. Qiu, D. R. Paul, W.J. Koros, Physical aging of 6FDA-based polyimide membranes monitored by gas permeability, Polymer 52 (2011) 3374-3380.

[59] C. Staudt-Bickel, W. J. Koros, Improvement of CO_2/CH_4 separation characteristics of polyimides by chemical crosslinking, Journal of Membrane Science 155 (1999) 145-154.

[60] A. Shimazu, T. Miyazaki, M. Maeda, K. Ikeda, Relationships between the chemical structures and the solubility, diffusivity, and permselectivity of propylene and propane in 6FDA-based polyimides, Journal of Polymer Science: Part B: Polymer Physics 38 (2000) 2525-2536.

[61] Y. Hirayama, T. Yoshinaga, S. Nakanishi, Y. Kusuki, “Relation between gas permeabilities and structure of polyimides”, in B.D. Freeman, I. Pinnau, Polymer membranes for gas and vapor separation: chemistry and materials science; ACS Symposium Series; Washington, DC. : American Chemical Society, 1999, pp: 194-214.

[62] S. H. Park, K. J. Kim, W. W. So, S. J. Moon, S. B. Lee, Gas Separation Properties of 6FDA-Based Polyimide Membranes with a Polar Group, Macromolecular Research 11 (2003) 157-162.

[63] H. Kawakami, M. Mikawa, S. Nagaoka, Formation of surface skin layer of asymmetric polyimide membranes and their gas transport properties, Journal of Membrane Science 137 (1997) 241-251.

[64] H. Kawakami, K. Nakajima, H. Shimizu, S. Nagaoka, Gas permeation stability of asymmetric polyimide membrane with thin skin layer: effect of polyimide structure, Journal of Membrane Science 212 (2003) 195–203.

[65] F. Hasanain, Z. Y. Wang, New one step synthesis of polyimides in salicylic acid, Polymer 49 (2008) 831-835.

[66] Y. K. Kim, J. M. Lee, H. B. Park, Y. M. Lee, The gas separation properties of carbon molecular sieve membranes derived from polyimides having carboxylic acid groups, Journal of Membrane Science 235 (2004) 139–146.

[67] S. Xiao, R. Y. M. Huang, X. Feng, Synthetic 6FDA-ODA copolyimide membranes for gas separation and pervaporation: Functional groups and separation properties, Polymer 48 (2007) 5355-5368.

[68] Y. Yampolskii, Polymeric gas separation membranes, Macromolecules 45 (2012) 3298−3311.

[69] N. A. Plate, Y. P. Yampolskii, “Relations between structure and transport properties for high free volume polymeric membranes ”, in D.R. Paul, Y. P. Yampolskii, Polymeric gas separation membranes, CRC Press, Boca Raton, FL., USA, 1994, pp:155-208.

[70] W. J. Koros, Simplified analysis of gas/polymer selective solubility behavior, Journal of Polymer Science, Part B: Polymer Physics Edition 23 (1985) 1611.

[71] V. I. Bondar, B. D. Freeman, I. Pinnau, Gas sorption and characterization of poly (ether-b-amide) segmented block copolymers, Journal of Polymer Science, Part B: Polymer Physics 37 (1999) 2463.

[72] H. Lin, B. D. Freeman, Materials selection guidelines for membranes that remove CO_2 from gas mixtures, Journal of Molecular Structure 739 (2005) 57–74.

[73] G. Dong, H. Li, V. Chen, Plasticization mechanisms and effects of thermal annealing of Matrimid hollow fiber membranes for CO_2 removal, Journal of Membrane Science 369 (2011) 206-220.

[74] W. R. Vieth, Membrane systems: Analysis and Design, USA: Oxford University Press, 1988.

[75] K. S. Chang, C. C. Tung, K. S. Wang, K. L. Tung, Free volume analysis and gas transport mechanisms of aromatic polyimide membranes: A molecular simulation study, Journal Physical Chemistry B 113 (2009) 9821-9830.

[76] K. S. Chang, Y. H. Huang, K. R. Lee, K. L. Tung, Free volume and polymeric structure analyses of aromatic polyamide membranes: A molecular simulation and experimental study, Journal of Membrane Science 354 (2010) 93-100.

[77] S. V. Lyulin, A. A. Gurtovenko, S. V. Larin, V. M. Nazarychev, A. V. Lyulin, Microsecond atomic-scale molecular dynamics simulations of polyimides, Macromolecules 46 (2013) 6357−6363.

[78] K. Tanaka, N. Islam, M. Kido, H. Kita, K. Okamoto, Gas permeation and separation properties of sulfonated polyimide membranes, Polymer 47 (2006) 4370–4377.

[79] M. Askari, T. S. Chung, Natural gas purification and olefin/paraffin separation using thermal cross-linkable copolyimide/ZIF-8 mixed matrix membranes, Journal of Membrane Science 444 (2013) 173–183.

List of Figures:

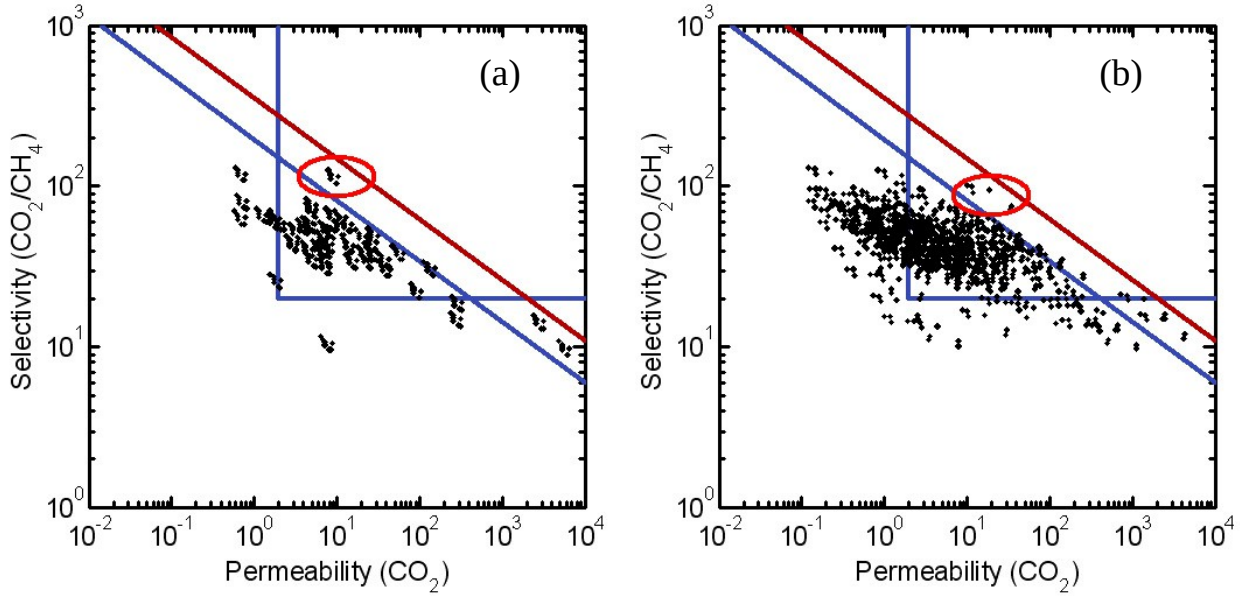
(a)
(b)
Selectivity (CO_2/CH_4)
Permeability (CO_2)
10^0
10^1
10^2
10^3
10^{-2}
10^{-1}
10^4

Figure 1

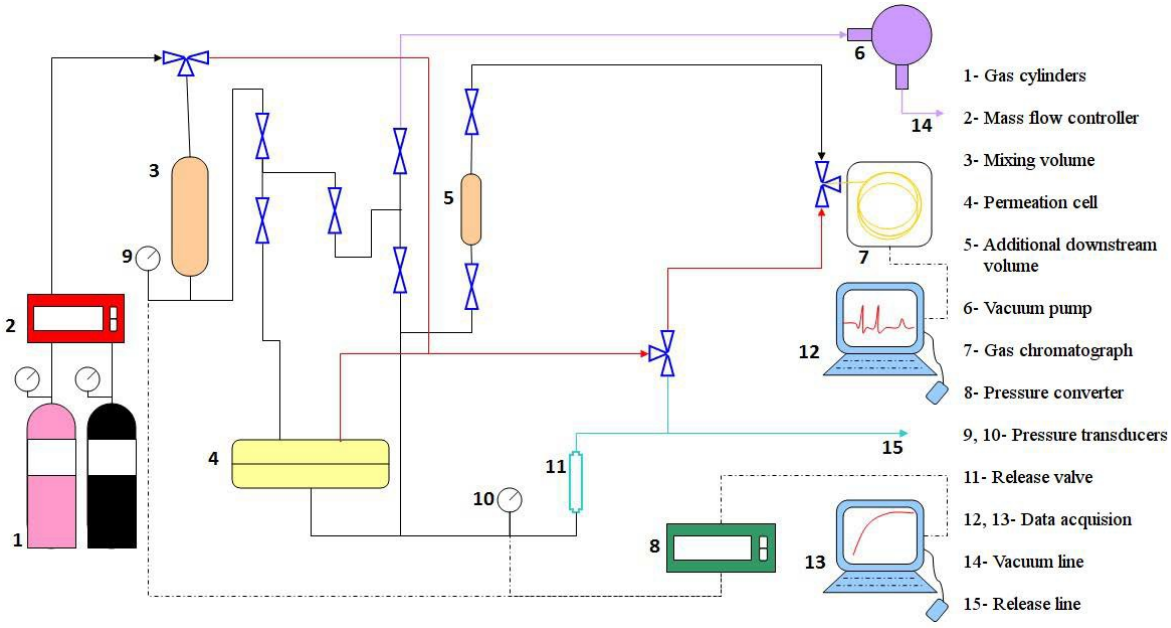
1- Gas cylinders
2- Mass flow controller
3- Mixing volume
4- Permeation cell
5- Additional downstream volume
6- Vacuum pump
7- Gas chromatograph
8- Pressure converter
9, 10- Pressure transducers
11- Release valve
12, 13- Data acquision
14- Vacuum line
15- Release line

Figure 2

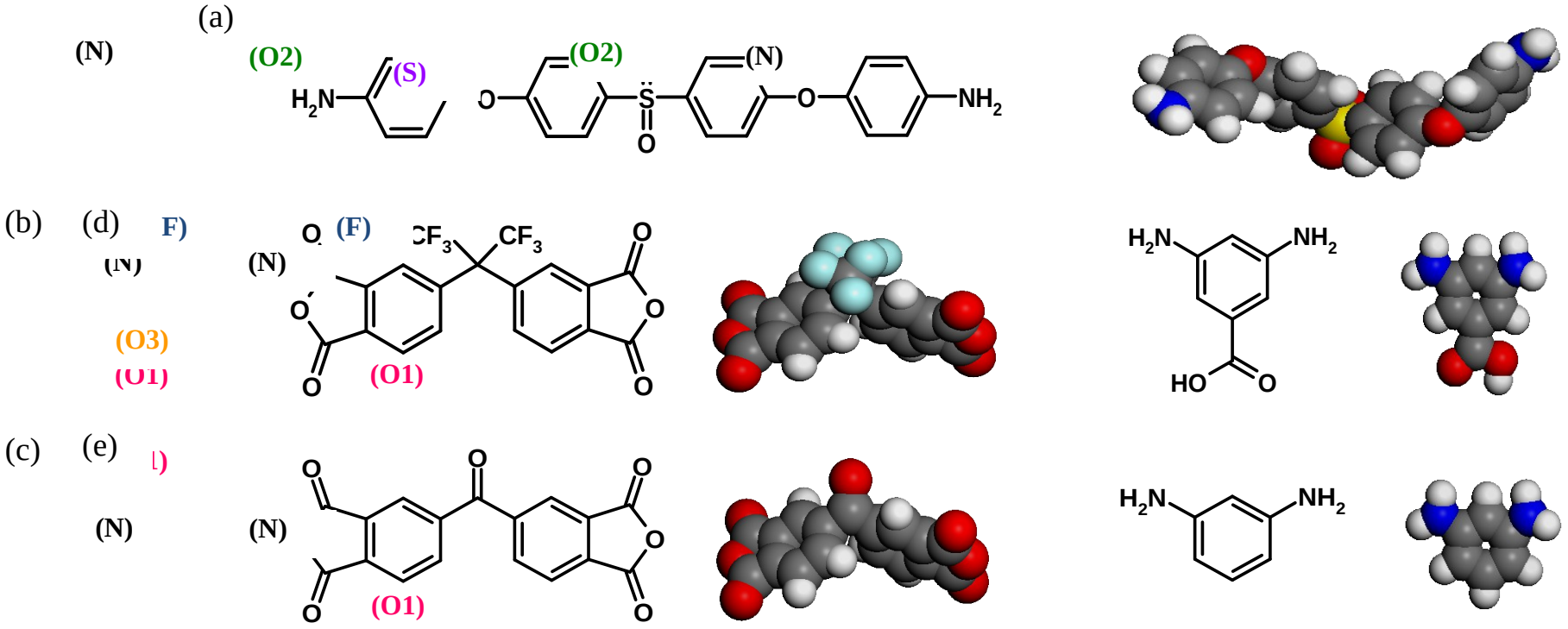
(a)
(N)
(O2)
(S)
(O2)
(N)
H_2N
O
O
O
NH_2
(b)
(d)
F)
(N)
O
(F)
CF_3
CF_3
O
O
O
O
(O3)
(O1)
(O1)
H_2N
NH_2
HO
O
(c)
(e)
l)
(N)
(N)
O
O
O
O
O
O
(O1)
H_2N
NH_2

Figure 3

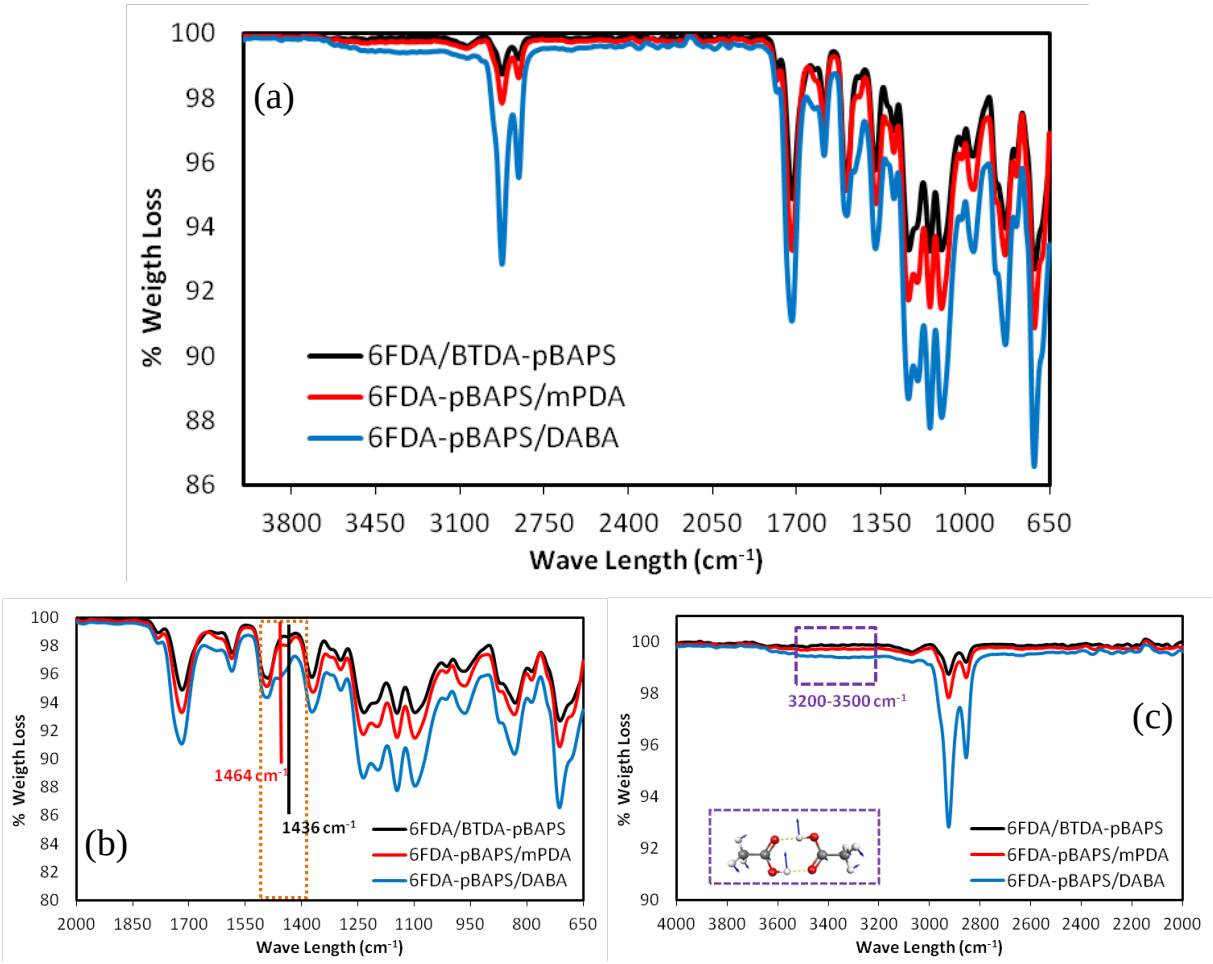
(a)
% Weigth Loss
Wave Length (cm-1)
6FDA/BTDA-pBAPS
6FDA-pBAPS/mPDA
6FDA-pBAPS/DABA
(b)
1464 cm-1
1436 cm-1
(c)
3200-3500 cm-1

Figure 4

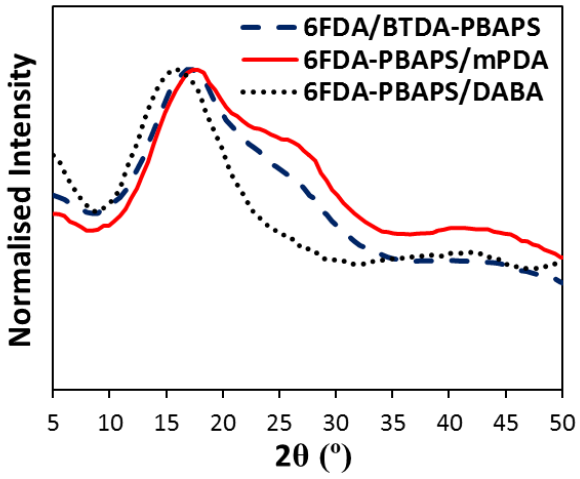
6FDA/BTDA-PBAPS
6FDA-PBAPS/mPDA
6FDA-PBAPS/DABA
Normalised Intensity
5
10
15
20
25
30
35
40
45
50
2θ (°)

Figure 5

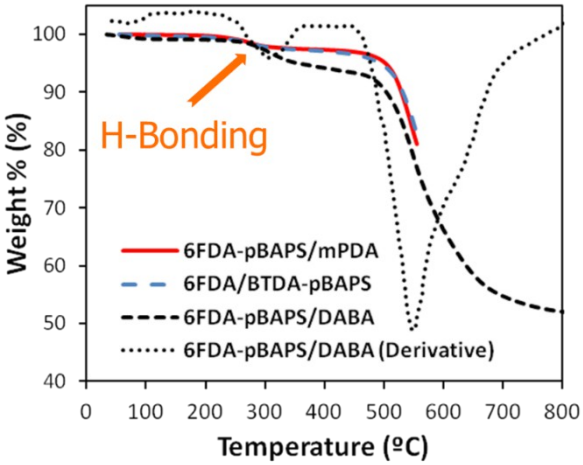
H-Bonding
Weight % (%)
Temperature (ºC)
6FDA-pBAPS/mPDA
6FDA/BTDA-pBAPS
6FDA-pBAPS/DABA
6FDA-pBAPS/DABA (Derivative)
100
90
80
70
60
50
40
0
100
200
300
400
500
600
700
800

Figure 6

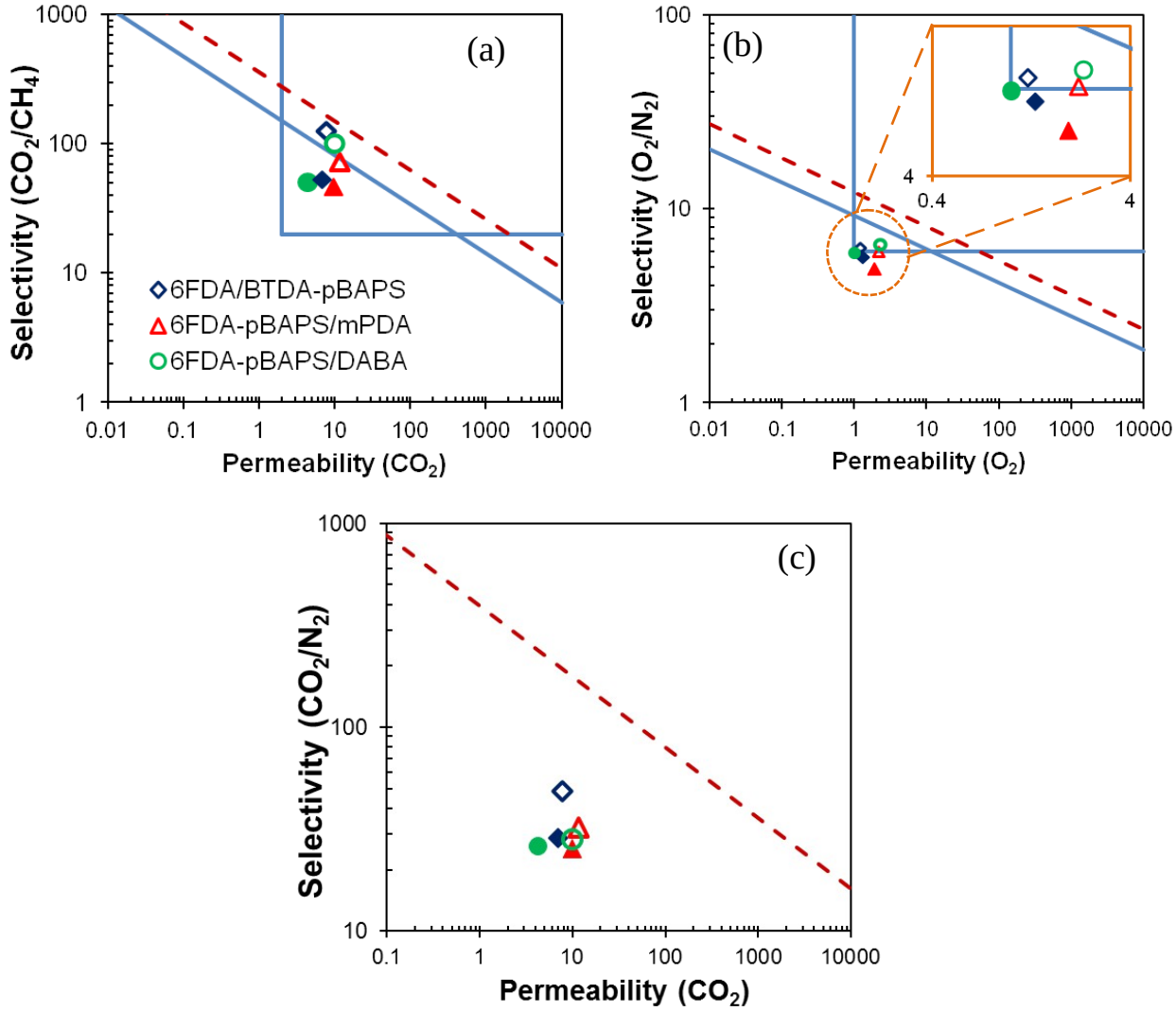
(a)
Selectivity (CO_2/CH_4)
Permeability (CO_2)
6FDA/BTDA-pBAPS
6FDA-pBAPS/mPDA
6FDA-pBAPS/DABA
(b)
Selectivity (O_2/N_2)
Permeability (O_2)
(c)
Selectivity (CO_2/N_2)
Permeability (CO_2)

Figure 7

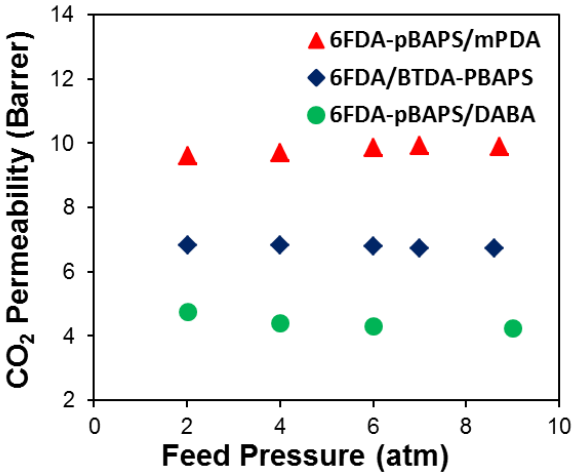
6FDA-pBAPS/mPDA
6FDA/BTDA-PBAPS
6FDA-pBAPS/DABA
CO_2 Permeability (Barrer)
Feed Pressure (atm)
14
12
10
8
6
4
2
0
2
4
6
8
10

Figure 8

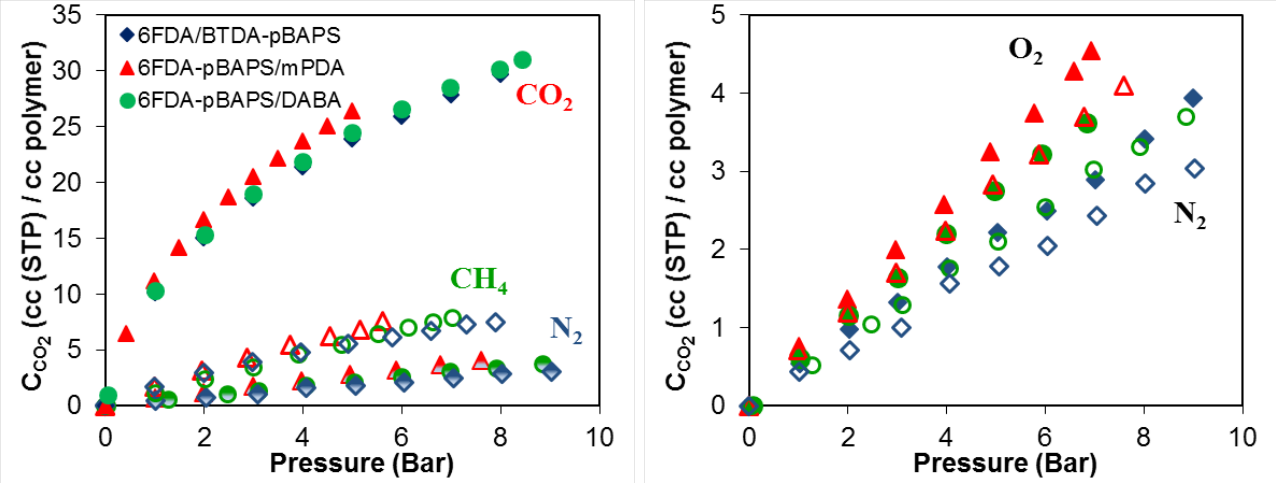
6FDA/BTDA-pBAPS
6FDA-pBAPS/mPDA
6FDA-pBAPS/DABA
CO2
CH4
N2
C_CO2 (cc (STP) / cc polymer)
Pressure (Bar)
O2
N2
C_CO2 (cc (STP) / cc polymer)
Pressure (Bar)

(a) (b)

Figure 9

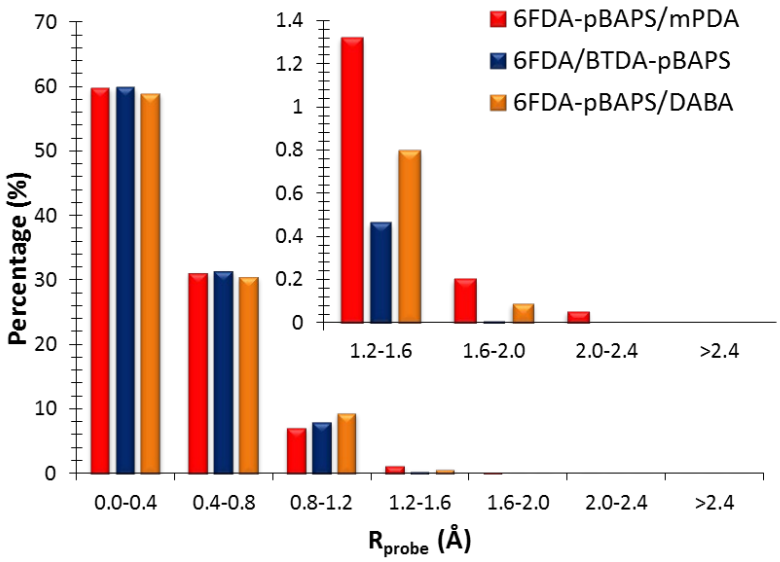
6FDA-pBAPS/mPDA
6FDA/BTDA-pBAPS
6FDA-pBAPS/DABA
Percentage (%)
70
60
50
40
30
20
10
0
0.0-0.4
0.4-0.8
0.8-1.2
1.2-1.6
1.6-2.0
2.0-2.4
>2.4
R probe (Å)
1.4
1.2
1
0.8
0.6
0.4
0.2
0
1.2-1.6
1.6-2.0
2.0-2.4
>2.4

Figure 10

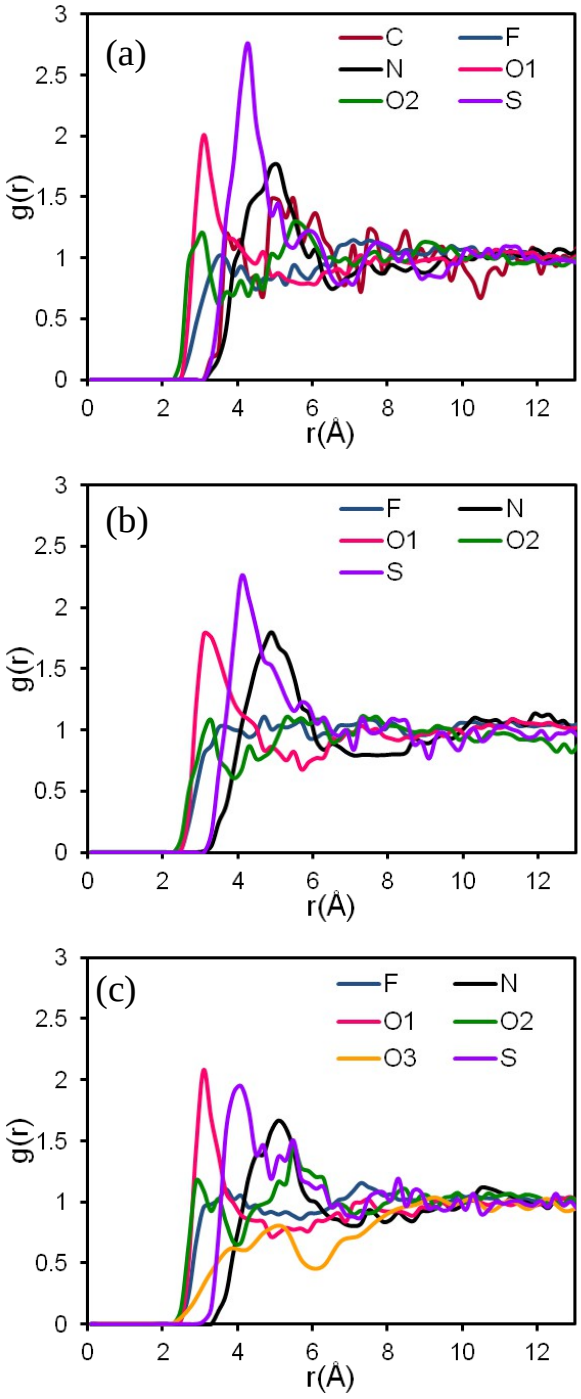

Figure 11

List of Tables:

Table 1

Monomer	Molecular Weight (g/mol)	Melting Point (°C)	Purity	Supplier
6FDA	444.25	244	≥ 99%	Aldrich
BTDA	322.23	220-223	> 97%	Merck
pBAPS	432.5	194-196	≥ 98%	TCI America
mPDA	108.14	64-66	≥ 99%	Aldrich
DABA	152.15	235-238	≥ 98%	Aldrich

Table 2

Properties		6FDA/BTDA-pBAPS	6FDA-pBAPS/mPDA	6FDA-pBAPS/DABA
Tg (ºC)	Exp.	276	285	287
	Sim.	290	280	331
d-spacing (Å)	Exp.	5.19	5.04	5.62
	Sim.	5.56	5.51	6.08
Density (g/cm^3)	Exp.[a]	1.387	1.400	1.419
	Sim.[b]	1.349	1.366	1.391
R_g(Å)	Sim.	36.6	29.0	25.6
FFV	Sim.	0.193	0.187	0.189
δ $(J/cm^3)^{1/2}$	Sim.	16.23	13.84	15.63
M_W (g/mol)	Exp.	87 000	102 000	58 000

[a] at 23ºC. [b] at 35ºC.

Table 3

Polyimide	Tg
6FDA-mPDA	286[a], 296[a], 297[b], 301[c], 305[d], 315[e]
6FDA-DABA	273[f], 309[g], 348[h]
6FDA-pBAPS	267[i] 278[f], 282[j], 299[k]
BTDA-pBAPS	289[k]

[a]Ref. 57, [b]Ref. 58, [c]Ref. 19, [d]Ref. 59, [e]Ref. 15, [f]Ref. 60, [g]Ref. 61, [h]Ref. 62, [i]Ref. 63, [j]Ref. 64, [k]Ref. 65.

Table 4

Polyimide	Permeability Coefficient (Barrer[a])				Ideal Selectivity (α)			
	CO_2[b]	CH_4[b]	O_2[b]	N_2[b]	CO_2/CH_4	CO_2/N_2	O_2/N_2	
6FDA/BTDA-pBAPS	7.76	0.06	1.20	0.19	126	48.5	6.32	GCM
	6.98[c]	0.13[d]	1.32[e]	0.23[e]	51.9	28.6	5.63	Exp.
6FDA-pBAPS/mPDA	11.6	0.16	2.18	0.36	72.6	32.2	6.06	GCM
	9.91[c]	0.21[d]	1.94[e]	0.39[e]	47.2	25.4	4.97	Exp.
6FDA-pBAPS/DABA	9.84	0.097	2.29	0.35	101	28.1	6.46	GCM
	4.25[f]	0.088[e]	1.00[e]	0.17[e]	48.3	26.1	5.93	Exp.

[a] Barrer=10^{-10} cm^3STP.cm / cm^2.s.cmHg; at 35ºC and [b] 10 bar; [c] 8.6 bar; [d] 4 bar; [e] 2 bar, [f] 9 bar.

Table 5

Polyimide	Sorption Coefficient (cm^3 (STP)/cm^3.bar)				Sorption Selectivity (α_S)		
	CO_2[a]	CH_4[a]	O_2[b]	N_2[b]	CO_2/CH_4	O_2/N_2	
6FDA/BTDA-pBAPS	3.62	1.29	2.13	1.21	2.81	1.76	**Sim.**
	3.33	0.88	0.46	0.37	3.78	1.24	**Exp.**
6FDA-pBAPS/mPDA	5.07[c]; 3.91	1.87[c]; 1.48	1.88	1.19	2.71; 2.64	1.58	**Sim.**
	5.29[c]	1.31[c]	0.69	0.61	4.04	1.13	**Exp.**
6FDA-pBAPS/DABA	3.80	1.45	1.76	1.14	2.62	1.54	**Sim.**
	3.39	1.09	0.57	0.43	3.11	1.33	**Exp.**

[a] at 35°C and 8 bar; [b] at 35°C and 2 bar ; [c] at 35°C and 5 bar;

Table 6

Polyimide	k_D (cm^3 (STP)/cm^3 polymer.bar)	C'_H (cm^3 (STP)/cm^3 polymer)	b (bar^{-1})
6FDA/BTDA-pBAPS	1.473	21.26	0.676
6FDA-pBAPS/mPDA	2.202	18.82	0.940
6FDA-pBAPS/DABA	1.443	22.49	0.635

Table 7

Polyimide		$S(CO_2)^a$	$S(CH_4)^a$	$\alpha_S(CO_2/CH_4)$
6FDA/BTDA-pBAPS	Single	3.04	1.29	2.37
	Mixed	5.26[b]	0.24[b]	21.9
6FDA-pBAPS/mPDA	Single	2.95	1.18	2.50
	Mixed	4.91[b]	0.34[b]	14.4
6FDA-pBAPS/DABA	Single	3.16	0.93	3.40
	Mixed	4.44[b]	0.37[b]	12.0

[a] at 35°C and 10 bar; [b] at 35°C and 5 bar

Graphical Abstract

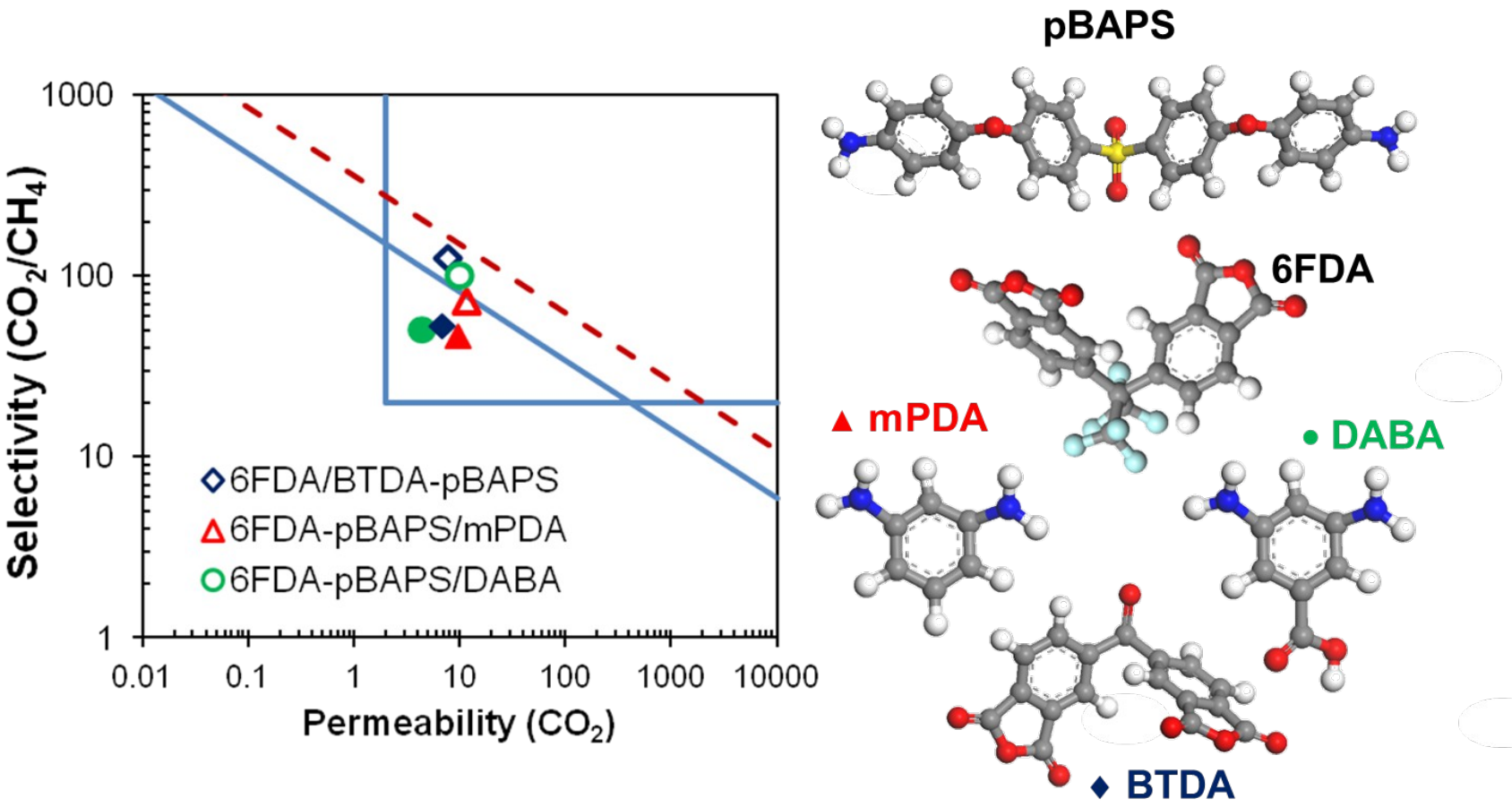

Supporting information for

NOVEL CO-POLYIMIDES CONTAINING A SULFONE GROUP FOR CO_2 SEPARATION

Sadiye Velioğlu, M. Göktuğ Ahunbay, S. Birgül Tantekin-Ersolmaz

Istanbul Technical University, Department of Chemical Engineering,

Maslak, Istanbul 34469, TURKEY

a) FTIR analysis

The FTIR spectra of polyamic acid and final co-polyimide for 6FDA/BTDA-pBAPS, 6FDA-pBAPS/mPDA and 6FDA-pBAPS/DABA synthesis are shown in Figure S.1 (a), (b), and (c), respectively. Characteristic absorption peaks of amic acid are NH-C stretching at 3525, 3522 and 3482 cm^{-1} wavelength, O-H (-COOH) stretching at 2934, 2933 and 2935 cm^{-1} wavelength, C=O (-COOH) stretching at 1633, 1635 and 1633 cm^{-1} wavelength. During the imidization step, the amic acid peaks disappear and characteristic imide peaks appear at 1722, 1726 and 1726 cm^{-1} wavelengths for C=O symmetric and asymmetric stretching and at 1374, 1373 and 1375 cm^{-1} wavelength for C-N stretching.

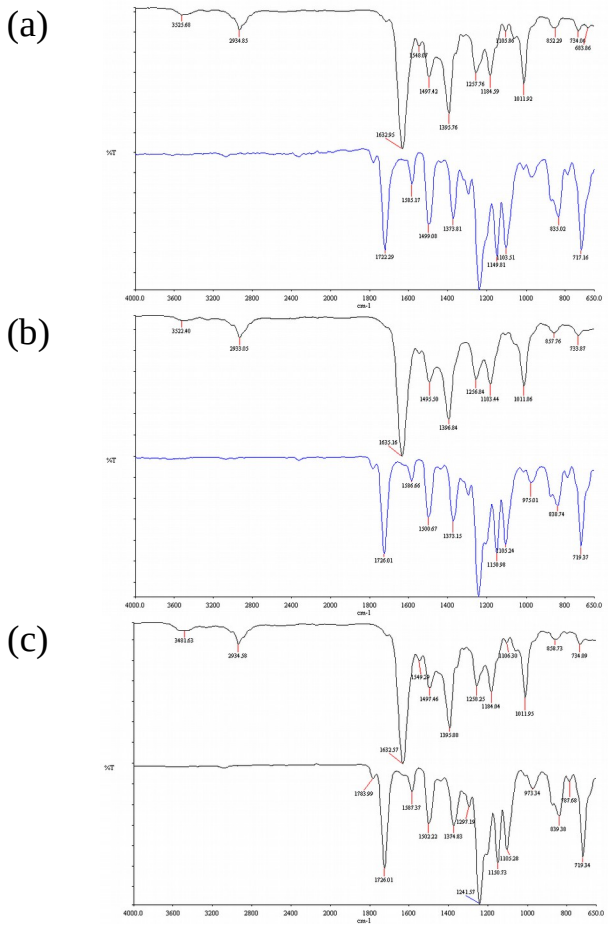

Figure S.1 FTIR spectrums of (a) 6FDA/BTDA-pBAPS, (b) 6FDA-pBAPS/mPDA and (c) 6FDA-pBAPS/DABA co-PIs. (top: polyamic acid and bottom: polyimide reaction steps).

b) TGA mass loss data

Table S.1 Mass Loss of 6FDA/BTDA-pBAPS, 6FDA-pBAPS/mPDA and 6FDA-pBAPS/DABA co-polyimides derived from TGA thermograms

Polyimide	Cumulative Mass Loss at (starting from 50ºC) (%)								
	100ºC	150 ºC	202 ºC	250 ºC	300 ºC	350 ºC	400 ºC	450 ºC	500 ºC
6FDA/BTDA-pBAPS	0.168	0.306	0.474	0.954	2.138	2.608	2.899	3.478	5.370
6FDA-pBAPS/mPDA	0.045	0.107	0.239	0.816	2.069	2.463	2.662	3.021	4.723
6FDA-pBAPS/DABA	0.769	0.863	0.928	1.179	2.685	4.869	5.795	6.642	9.394